energies

MDPI

Article

Sedimentary Characteristics and Their Controlling Factors of Lower Cretaceous Fan Deltas in Saidong Sub-Sag of Saihantala Sag, Erlian Basin, Northeastern China

Bo Yan [1,2], Hongqi Yuan [2,*], Xuanlong Shan [1], Tianqi Zhou [2] and Shengfei Liu [2]

[1] College of Earth Sciences, Jilin University, Changchun 130061, China
[2] School of Geosciences, Northeast Petroleum University, Daqing 163318, China
* Correspondence: yuan_flag@163.com; Tel.: +86-189-4599-5279

Abstract: Fan deltas of the Lower Cretaceous area in Saihantala sag, Erlian Basin have been identified as major petroleum exploration opportunities. The sedimentary evolution is, however, still debatable, which hinders insights into its controlling factors. This research employed new core observations, thin section observations, and grain size analyses of 28 wells in the Saidong sub-sag, together with numerous borehole and seismic data points, to explore lithofacies types, subfacies, and microfacies characteristics, thus leading to a further investigation of the sedimentary facies evolution of the sag and its controlling factors. The findings showed there are 3 categories, 12 sub-categories, and 20 fine lithofacies types in the Saidong sub-sag. Additionally, various sand-conglomerate lithofacies were characterized by lower composition and texture maturity. With dentate-shaped, box-bell-shaped, and other morphological well-logging responses, fan deltas were mostly developed in the A'ershan Formation and the Tengge'er Formation, which could be subdivided into three subfacies and eight microfacies. Given the sedimentary features and lithofacies characteristics of each microfacies, it can be determined that three main stages occurred in formations from the A'ershan to the Tengge'er: the water transgression, the water oscillation, and the water regression. Moreover, fan delta deposits were regulated primarily by semi-arid hygrothermal and semi-arid paleoclimate and paleotectonic factors.

Keywords: Saidong sub-sag; lower cretaceous; fan delta; sedimentary microfacies; controlling factors

Citation: Yan, B.; Yuan, H.; Shan, X.; Zhou, T.; Liu, S. Sedimentary Characteristics and Their Controlling Factors of Lower Cretaceous Fan Deltas in Saidong Sub-Sag of Saihantala Sag, Erlian Basin, Northeastern China. *Energies* **2022**, *15*, 8373. https://doi.org/10.3390/en15228373

Academic Editor: Reza Rezaee

Received: 10 October 2022
Accepted: 7 November 2022
Published: 9 November 2022

1. Introduction

Since Holmes put forward the concept of the fan delta in 1965, it has come to be regarded as a typical alluvial fan that routes terrestrial sediments from adjacent highlands into quiet water. Growing awareness over the controlling factors in the formation of fan deltas has revealed that the distance of sediment transport, the depth of sedimentary water, the paleoclimate, and the paleogeomorphology of the sedimentation cause significant changes in its sedimentary characteristics and fan delta evolution. All these factors can influence the geometry of fan deltas and their architectural elements. They can also impact the predominance of different depositional processes, determining distributions of grains and sedimentary structures, and thereby lithofacies [1–13]. Previous studies indicate that strong tectonic activities, arid-semiarid climate, sufficient material supply, and rapid accumulation account for fan deltas, which are usually composed of fan delta plain, fan delta front, and prodelta [14–17]; tectonic activities in continental rift basins generate accommodation and dominate fan delta sedimentary architectures [18–21] and sequence evolution [22–25], and variations in the fault activity bring about changes of the depocenter location in space and time [26]; climate changes influence the accommodation by varied lake depths, and thus stratigraphic architectural patterns [19,25,27,28]. What is more, sequence types act as a function of the balance between tectonic subsidence and sediment supply. In active rift basins, variations in tectonic subsidence govern the growth or reduction in accommodation [28].

Given different schemes for their classification, fan deltas can be classified as "mountain style" as well as "fan style" based on their development locations [29], as "arid fan delta" or "humidity fan delta" depending on the climatic conditions, as "progradational delta", "aggradational delta", or "retrogradational delta" [30] by the sedimentary mode, as "river-dominated fan delta", "wave-dominated fan delta", or "tide-dominated fan delta" based on the control effect of water on fan sedimentation [31], and also as "large-scale fan delta" or "small-scale fan delta" according to its vertical extension distance [2,32].

The Erlian Basin has attracted a great deal of interest in fan delta studies, mostly concentrating on the background of its sedimentation [33,34], sedimentary characteristics [35], sedimentary patterns [36–38], sedimentary sequences [30,39,40], reservoir features [41,42], lithofacies [43,44], as well as fan delta subfacies, microfacies, and their evolution [45–53]. The sedimentary facies pattern of fan deltas in the Erlian Basin [54] and the division scheme of sedimentary facies in the Saihantala sag have been investigated after decades of research [55,56]. However, much work was done on the whole Erlian Basin and the Saihantala sag, but the accuracy of sedimentary facies' division was rather limited. Additionally, the relationship between sedimentation and structure evolution was seldom emphasized, which is believed to play a critical role in the fan delta distribution as well as the subaqueous distributary channel microfacies.

A thorough understanding of lithofacies and sedimentary facies of fan deltas in the Erlian Basin can help to relate the sedimentary facies evolution to the basin structure evolution. Based on new core observations, the particle size analysis of 28 drilling wells, as well as interpretation of drilling, seismic exploration data, and borehole data of the A'ershan Formation and the Tengge'er Formation of the Lower Cretaceous Saidong sub-sag, Saihantala sag, the current work manages to identify distinct types of lithofacies and the characteristics of sedimentary facies of fan deltas in the Erlian Basin and figure out the sedimentary facies evolution and planar distribution of the Saidong sub-sag. These findings, together with the structure evolution analysis, have a clear vision of the sedimentary controlling factors of fan deltas in the Saidong sub-sag and will propel the insights into the sedimentary characteristics of fan deltas in other potential areas of the Erlian Basin.

2. Geological Setting

The Erlian Basin is located in the Great Khingan fold belt of Inner Mongolia of NE China. The Mesozoic–Cenozoic basin formed at the suture zone of the Asian and Siberia plates (Figure 1a), which is controlled by the tectonic stress of the Yanshanian tensional uplift [57,58]. This basin consists of five depressions of Manit, Unit, Ulanqab, Chuanjing, and Tengge'er, and three uplifts of Bayinbaolig, Sunit, and Wenermiao [59]. The Saihantala sag lies in the southern-central part of the Erlian Basin (Figure 1b), which is approximately 100 km long from north to south and about 19–27 km wide, with a total area of about 2300 km^2. The sag gently shows an "S" shape and its formation has always been subject to the subduction of the Pacific plate to the Eurasian plate [56,60].

The Saihantala sag can be subdivided into the western sub-sag belt, central fault belt, eastern sub-sag belt, and eastern steep slope belt. The Saidong sub-sag is located in the eastern Saihantala sag with a total area of about 450.65 km^2 (Figure 1c), which shows a long-narrow NE trend. Due to the activation of the syndepositional strike-slip faults such as the Xilin fault and Zhabu fault, the Saidong sub-sag became a graben-type sag (Supplementary Figures S1 and S2), which is the sedimentation and subsidence center of the entire Saihantala sag.

Triassic strata are absent in most areas of the Erlian Basin [58]. The Lower Cretaceous fan deltas, which mainly comprise thick glutenite, pebbled sandstone, coarse sandstone, and mudstone (Figure 2), mainly developed in the sedimentary strata of the A'ershan Formation (K_1ba), Tengge'er Formation (K_1bt), and Saihantala Formation (K_1bs) from bottom to top. During the deposition of the Upper Jurassic, the sag extended about 26.92 km. During the deposition of the A'ershan Formation (K_1ba), ranging from 34 to 405 m, the sag length extended about 27.39 km, indicating the intense fault activities as

well as related significant subsidence and deposition. The thickness of the first member of the Tengge'er Formation (K_1bt_1) was about 28–598 m and the total length was about 27.48 km. During this period, the large flooding deposit was mainly controlled by the normal faults in the eastern margin. During the deposition of the second member of the Tengge'er Formation (K_1bt_2), the thickness was 147–1591 m and the total length was about 28.58 km. The uplift of the central horst caused the westward propagation of the subsidence center of the western trough, which indicated that the controlling of faults on basin sedimentation was weakened. This was also supported by the minor change of the subsidence center of the eastern trough. During the sedimentary period of the Saihantala Formation (K_1bs), the sag length was about 29.22 km and its thickness decreased to about 55–380 m [61,62]. The fault depression of the basin was replaced by regional subsidence, which was mainly characterized by overlap deposition, indicating that the subsidence centers of the sub-sag used to move to the east and west parts, respectively, and the influence of fault activities on the basin nearly disappeared (Figure 3, Figures S1 and S2).

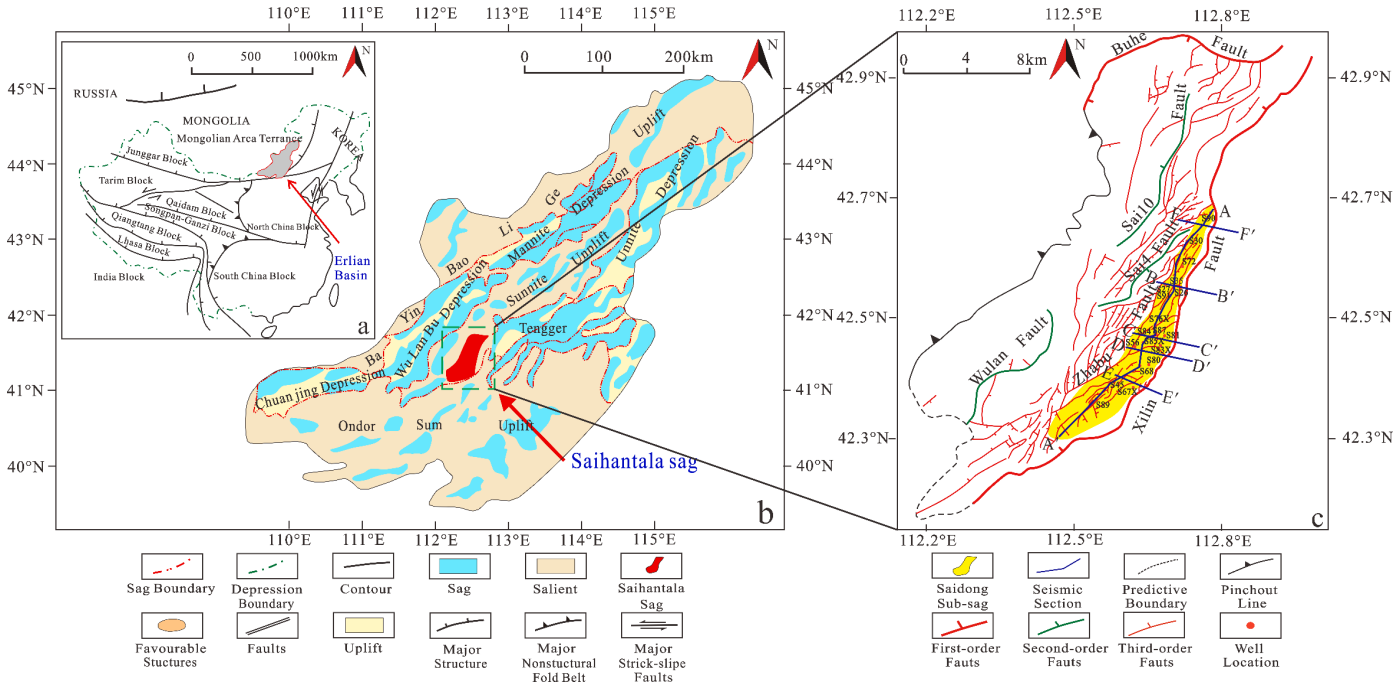

Figure 1. Simplified diagram of the structural area of Saihantala sag in Erlian Basin [62,63]. (**a**) The tectonic position of the Erlian Basin. (**b**) Structural unit division of Erlian Basin. (**c**) Fault distribution characteristics of Saihantala sag and Saidong sub-sag.

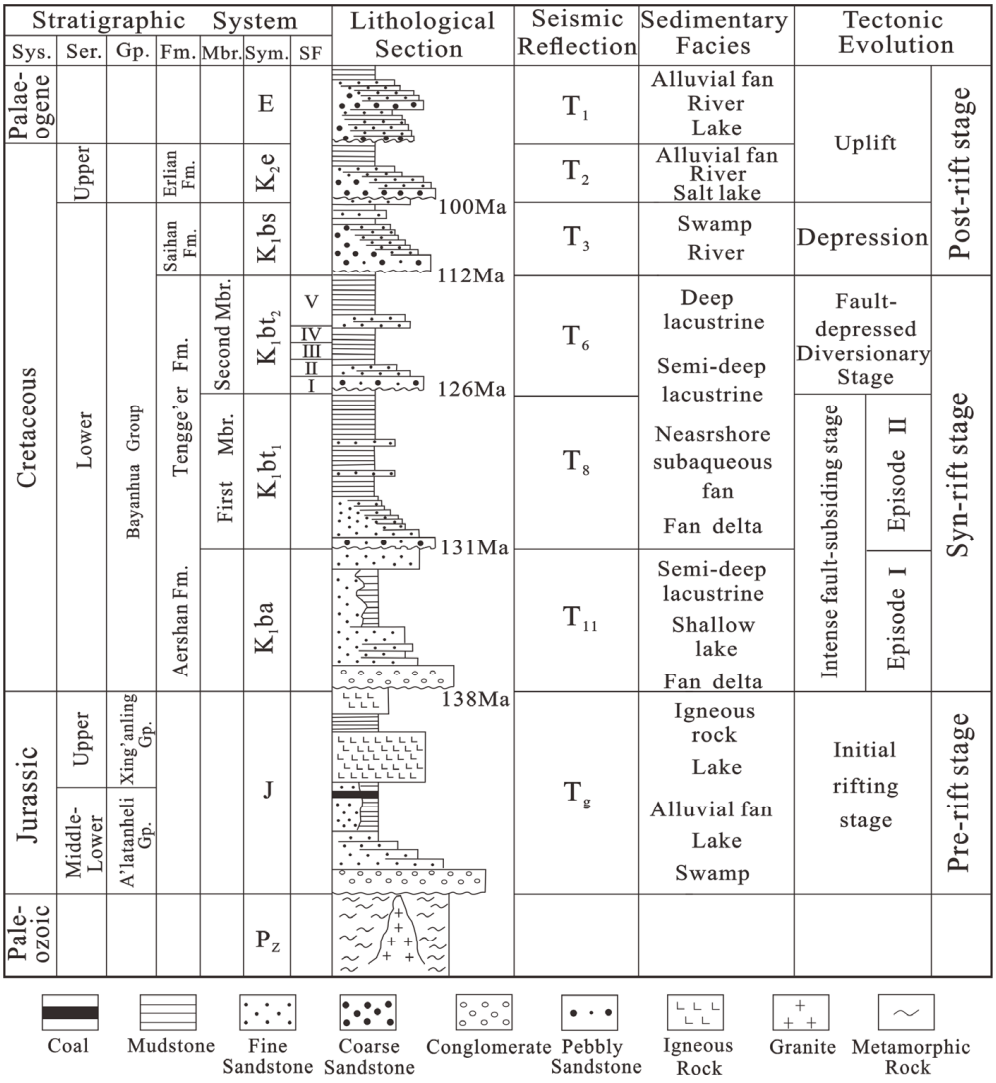

Figure 2. The stratigraphic succession map of Saihantala sag [58]. Abbreviations: Sys.: System; Ser.: Series; Gp.: Group; Fm.: Formation; Mbr.: Member; Sym.: Symble; SF: Sand Formation.

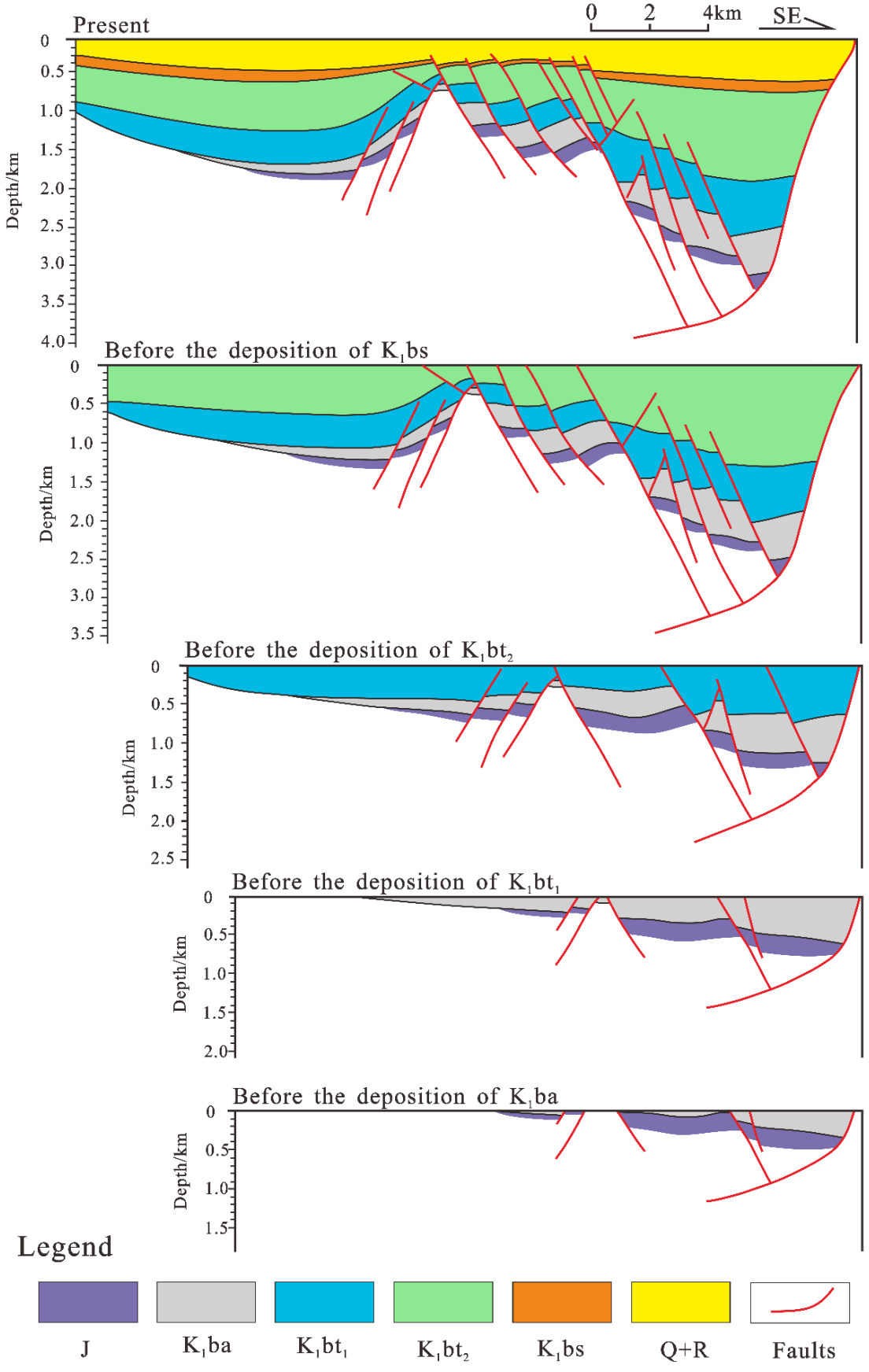

Figure 3. Tectonic evolution map of Saidong sub-sag in Saihantala sag, Erlian Basin [61,62].

3. Data and Methods

3.1. Data

The datasets used in the Saidong sub-sag consisted of seismic data, well data, borehole data, and core photographs. The well data were derived from 28 wells with logging curves, among which lithology logs were selected to investigate the depositional systems. All these data were collected from the Huabei Oilfield Branch of Petro China.

3.2. Methods

Different types of depositional systems were revealed by distinctive geometries of well-logging curves and their associated sedimentary structures in cores. The tectonic evolution (Figure 3) was modified after Fu et al. [62], based on new core observations, the particle size analysis of 28 drilling wells, as well as the interpretation of drilling and borehole data of the A'ershan Formation and the Tengge'er Formation of the Lower Cretaceous Saidong sub-sag, Saihantala sag.

4. Results

4.1. Sedimentary Characteristics

4.1.1. Lithofacies Analysis and Interpretation

Each lithofacies usually responds to a specific sedimentary environment, which can serve as a hydrodynamic indicator amid the deposition [44]. This study performed core observation and grain size analysis together with sedimentary structure interpretation of 28 wells from the Saidong sub-sag of the Saihantala sag to characterize the lithofacies of Lower Cretaceous fan deltas. The results show lithofacies of Lower Cretaceous fan deltas can be divided into 3 types, 12 subtypes, and 20 fine types (Table 1, Figure 4).

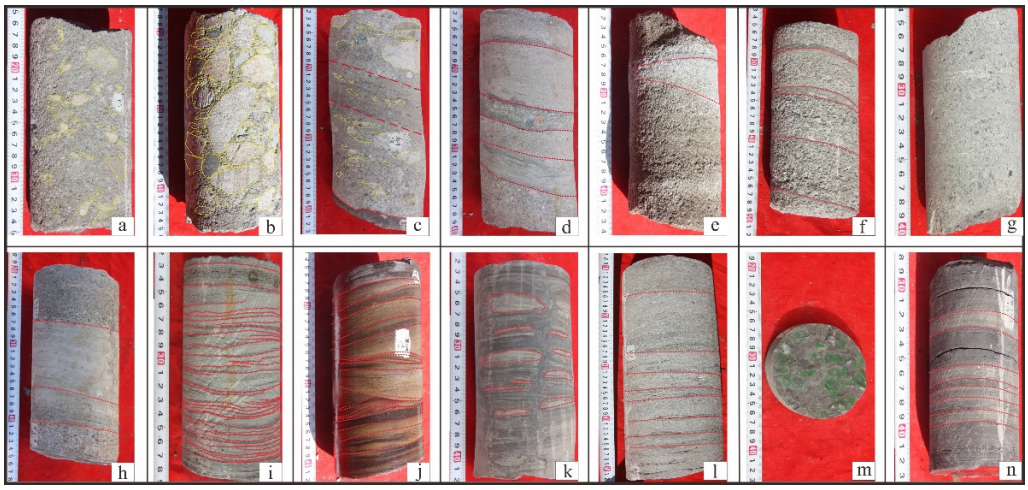

Figure 4. Lithofacies types of Saidong sub-sag in Saihantala sag, Erlian Basin. (**a**) Structureless clast-supported conglomerate, S27, 1658.42–1677.15 m; (**b**) Multi-order grain-supported conglomerate, S67X, 2378.33–2406.29 m; (**c**) Orientationally arranged conglomerate, S80, 2192.13–2192.29 m; (**d**) Graded conglomerate, S79, 1845.71–1845.97 m; (**e**) Trough cross stratified conglomerate, S63, 1333.87–1356.43 m; (**f**) Parallel-bedded conglomerate, S48, 1510.24–1535.01 m; (**g**) Structureless clast-supported sandstone, S12, 2280.71–2297.24 m; (**h**) Graded sandstone, S33, 1809.54–1835.07 m; (**i**) Cross-bedded sandstone, S79 m, 1866.21–1882.93 m; (**j**) Wave cross fine-grained sandstone, S88, 2121.51–2149.44 m; (**k**) Lenticular-bedded muddy fine-grained sandstone, S68, 2177.21–2197.33 m; (**l**) Parallel-bedded fine-silty sandstone, S33, 1865.37–1910.68 m; (**m**) Sandy mudstone, S44, 1883.72–1883.86 m; (**n**) Gray mudstone, S84, 2040.31–2055.34 m.

Table 1. Lithofacies types of the Lower Cretaceous Saidong sub-sag.

Type	Subtype	Fine Type
Conglomerate lithofacies	A Structureless clast-supported conglomerate	A1 Mud-supported conglomerate A2 Sand-supported conglomerate
	B Grain-supported conglomerate	B1 Multi-order grain-supported conglomerate B2 Single-order grain-supported conglomerate
	C Orientationally arranged conglomerate	C1 Imbricate granule conglomerate C2 Imbricate pebble conglomerate
	D Graded conglomerate	D1 Graded sand–mud filling conglomerate D2 Graded sand-filling conglomerate
	E Trough cross-bedded conglomerate	E1 Stratified mud–sand-supported conglomerate E2 Stratified sand-supported conglomerate
	F Parallel-bedded conglomerate	F1 Parallel-bedded mud-filling granule conglomerate
Sandstone lithofacies	G Structureless clast-supported sandstone	G1 Medium-coarse gravel sandstone
	H Graded sandstone	H1 Normal-graded sandstone H2 Inverse-graded sandstone
	I Cross-bedded sandstone	I1 Through cross medium-coarse sandstone I2 Wave cross fine-grained sandstone
	J Lenticular-bedded sandstone	J1 Lenticular-bedded muddy fine-grained sandstone
	K Parallel-bedded sandstone	K1 Parallel-bedded fine-silty sandstone
Mudstone lithofacies	L Mudstone	L1 Sandy mudstone L2 Gray mudstone

1. Conglomerate lithofacies

Conglomerate lithofacies developed in the Saidong sub-sag can be divided into six types based on different supporting structures and sedimentary structures, the structureless clast-supported conglomerate, grain-supported conglomerate, orientationally arranged conglomerate, graded bedded conglomerate, trough cross-bedded conglomerate, and parallel-bedded conglomerate lithofacies.

The structureless clast-supported conglomerate lithofacies (A) mainly consist of coarse and medium conglomerates with poor roundness and sorting characteristics. The structures of these lithofacies are mainly massive structures with minor bedding features, which are the main characteristics of the fan delta plain facies. Based on the matrix type of structureless clast-supported conglomerate lithofacies, it can be divided into mud-supported conglomerate (A1) and sand-supported conglomerate (A2, Table 1). The former was mostly developed in the mud-rich gravity flow sedimentary environment of the fan delta plain subfacies with fewer in the upper fan delta front [64]. The latter mainly formed under the alteration of sand-rich gravity flow and debris flow. The gravels are floated in the gray-brown sandstone grains.

The grain-supported conglomerate lithofacies (B) of the Lower Cretaceous fan deltas in the Saidong sub-sag are dominated by massive structures with minor sedimentary structures, which is consistent with the main feature of the fan delta plain subfacies or upper fan delta front [65]. Based on the sorting features of particles, it can be divided into two kinds of fine lithofacies: the multi-order grain-supported conglomerate (B1) and the single-order grain-supported conglomerate lithofacies (B2, Table 1). The former one features poorly mixed, sorted, and rounded conglomerate, with fine gravel and a sandy fill among medium and coarse gravels, which, matched with the gravity flow sedimentation, formed during the middle and late stages of the fan delta plain subfacies. The latter lithofacies is mainly composed of better sorting and rounded pebble-granule conglomerate, with point contact among particles mainly caused by developed pores and better connectivity. These lithofacies are common in subaqueous distributary channels of the fan delta front, resulting from stable hydrodynamic forces.

The orientationally arranged conglomerate lithofacies (C) of the Lower Cretaceous fan deltas in the Saidong sub-sag are mainly composed of well-sorted and rounded layered or imbricated pebble-granule conglomerate [65]. Based on different grain sizes, it can be subdivided into imbricate granule conglomerate (C1) and imbricate pebble conglomerate (C2, Table 1). Both of these two subfacies have point-contact particles with intergranular pores, primarily developed with traction flow in subaqueous distributary channels of the fan delta front.

Graded conglomerate lithofacies (D) of the Lower Cretaceous fan deltas in the Saidong sub-sag have similar features to the structureless clast-supported conglomerate lithofacies, yet with distinctive characteristics [66]. They are generally formed in fan delta plain channels. Based on the interstitial material, these lithofacies can be divided into two types of fine lithofacies as well: the graded sand–mud filling conglomerate (D1) and the graded sand-filling conglomerate (D2, Table 1). The former is developed in the gravity flow, and the latter is formed with the gradually weakened traction flow.

The trough cross-bedded conglomerate lithofacies (E) of Lower Cretaceous fan deltas in the Saidong sub-sag are mainly composed of gravity flow- and traction flow-induced moderately sorted and rounded pebble-granule conglomerate. It is consistent with the main features of the end of fan delta plain subfacies and the fan delta front subfacies. Based on the different supporting materials, it can be divided into two fine types of lithofacies (Table 1): the trough cross-bedded mud–sand-supported conglomerate (E1) and trough cross-bedded sand-supported conglomerate lithofacies (E2). The former one mostly developed at river channels amid the end of flooding. The latter one usually developed at the end of the fluvial deposition with the hydrodynamic force being gradually weakened, which represented the middle and lower parts of subaqueous distributary channels in the fan delta front [67].

The parallel-bedded conglomerate lithofacies (F, Table 1) of the Lower Cretaceous fan deltas in the Saidong sub-sag are mainly composed of mud-rich granule conglomerate with parallel bedding and directional alignment of gravel [68]. It is mostly developed at the wide sheet flood zone of the surface of the fans during flooding, or the river channels during the end of flooding. With the weakening water transport capacity, this lithofacies was caused by the gravity flow as well as the traction flow, characterizing the main deposition characteristic of the end of fan delta plain subfacies.

The various conglomerate lithofacies of the fan delta plain and the fan delta front are developed in the Lower Cretaceous area in Saidong sag, indicating that they were mostly controlled by the continuous subsidence during the development of the faulted-basin depression of the Saidong sag. This is also supported by the gradual changing of the sedimentary environment and the integrity of the sedimentary sequence of marginal facies.

2. Sandstone lithofacies

The sandstone lithofacies in the Saidong sub-sag can be divided into five types, including structureless clast-supported sandstone, graded sandstone, cross-bedded sandstone, lenticular-bedded sandstone, and parallel-bedded sandstone lithofacies.

Structureless clast-supported sandstone lithofacies of the Lower Cretaceous fan deltas in Saidong sub-sag (G, Table 1) feature medium sorting and grinding of medium-coarse sandstone, with a small amount of pebble, which is the major characteristic of fan delta front subfacies deposits. This lithofacies is mainly caused by sandy debris flow with intense hydrodynamic force. It is usually eroded in the upper part of the fan delta front and well-preserved in the lower part of the fan delta front.

Graded sandstone lithofacies of the Lower Cretaceous fan delta in Saidong sub-sag (H, Table 1) are characterized by fine-coarse sandstone, with high grain sorting and rounding [69]. These lithofacies' features are consistent with the main sedimentary characteristics of fan delta front subfacies. The normal-graded sandstone (H1) is mostly developed in the subaqueous distributary channel of fan delta front subfacies, and inverse-graded sandstone (H2) is mainly formed at the debouch bar of fan delta front subfacies.

Cross-bedding sandstone lithofacies of the Lower Cretaceous fan delta in the Saidong sub-sag (I, Table 1) are dominated by fine-grained sandstone, which is the main sedimentary

characteristic of fan delta front subfacies. It can be subdivided into two categories: trough cross-bedded medium-coarse sandstone (I1) and wave cross-bedded fine-grained sandstone (I2). The former lithofacies are mainly composed of gray-brown fine-medium sandstones with moderate sorting characteristics. It is formed by traction flow at subaqueous distributary channels of fan delta front subfacies. Wave cross-bedded fine-grained sandstone is usually composed of fine-grained sandstones with argillaceous laminae and small interbedded beddings. These lithofacies are formed in traction flow among subaqueous distributary channels or sand sheets in fan delta front subfacies [67].

Lenticular-bedded sandstone lithofacies of the Lower Cretaceous fan delta in Saidong sub-sag (J, Table 1) are characterized by a sand lens wrapped in the argillaceous layer, indicating sufficient sand and mud supply [69]. As the sediment transport distance increased, the gradually weakened hydrodynamic condition resulted in insufficient arenaceous supply, while the mud supply was still sufficient. These lithofacies usually developed in the mouth bar of fan delta front subfacies.

Parallel-bedded sandstone lithofacies of the Lower Cretaceous fan delta in Saidong sub-sag (K, Table 1) were dominated by silty-fine sandstone with argillaceous lamina and parallel bedding, caused by traction flow [69]. It is the major sedimentary characteristic of fan delta front subfacies, developing in sand sheets of the fan delta front.

The various sedimentary characteristics of fan delta front subfacies in the Saidong sub-sag were developed under the background of gradual weakening of hydrodynamic force, indicating that the formation and evolution of the Saidong sag entered the fault-depression transformation period. It has relatively stable sedimentation and the water level gradually deepened.

3. Mudstone lithofacies

Mudstone lithofacies of the Lower Cretaceous fan delta in the Saidong sub-sag are characterized by gray mudstone that formed in the weak hydrodynamic environment, which is the main sedimentary characteristic of prodeltas [70]. Mudstone lithofacies (L, Table 1) can be subdivided into two categories: sandy mudstone (L1) and gray mudstone (L2). Sandy mudstone is mainly distributed in the interchannel areas, with sand-poor parallel bedding, and occasionally plant debris and conchostracan fossils are found. Gray mudstone is usually distributed in the subaquatic reductive environment with stable hydrodynamic conditions.

4.1.2. Detrital Component

The observation and semi-quantitative analysis of thin sections of 28 wells in the study area showed that feldspathic sandstone and feldspathic lithic sandstone were commonly developed in the Lower Cretaceous fan delta in the Saidong sub-sag. The quartzite lithic sandstone and granite lithic sandstone were developed with particle support. There are various cementation types such as thin-film cementation, pore cementation, and intergranular dissolved pores (Figures 5 and 6). During the A'ershan period (Figure 5), the debris components of braided channels in the fan delta plain subfacies were quite different from subaqueous distributary channels in the fan delta front subfacies. The content of lithoclast in fan delta plain subfacies was up to 54%, reflecting the characteristics of rapid accumulation of clastic sediments from near sources. The content of rigid particles such as quartz and feldspar in fan delta front subfacies was higher. The content of quartz particles ranged from 32% to 45%, and the feldspar reached 15% to 35%. The fan delta plain subfacies were less developed during the Member 1 of the Tengge'er period. The quartz content in the subaqueous distributary channel of the fan delta front was between 30% and 40% and the feldspar content ranged from 18% to 37%. The content of debris was up to 35%, which was less than that in the A'ershan period. The above data indicate that the higher the quartz and feldspar content, the greater the transport distance from the detrital sediment, and vice versa.

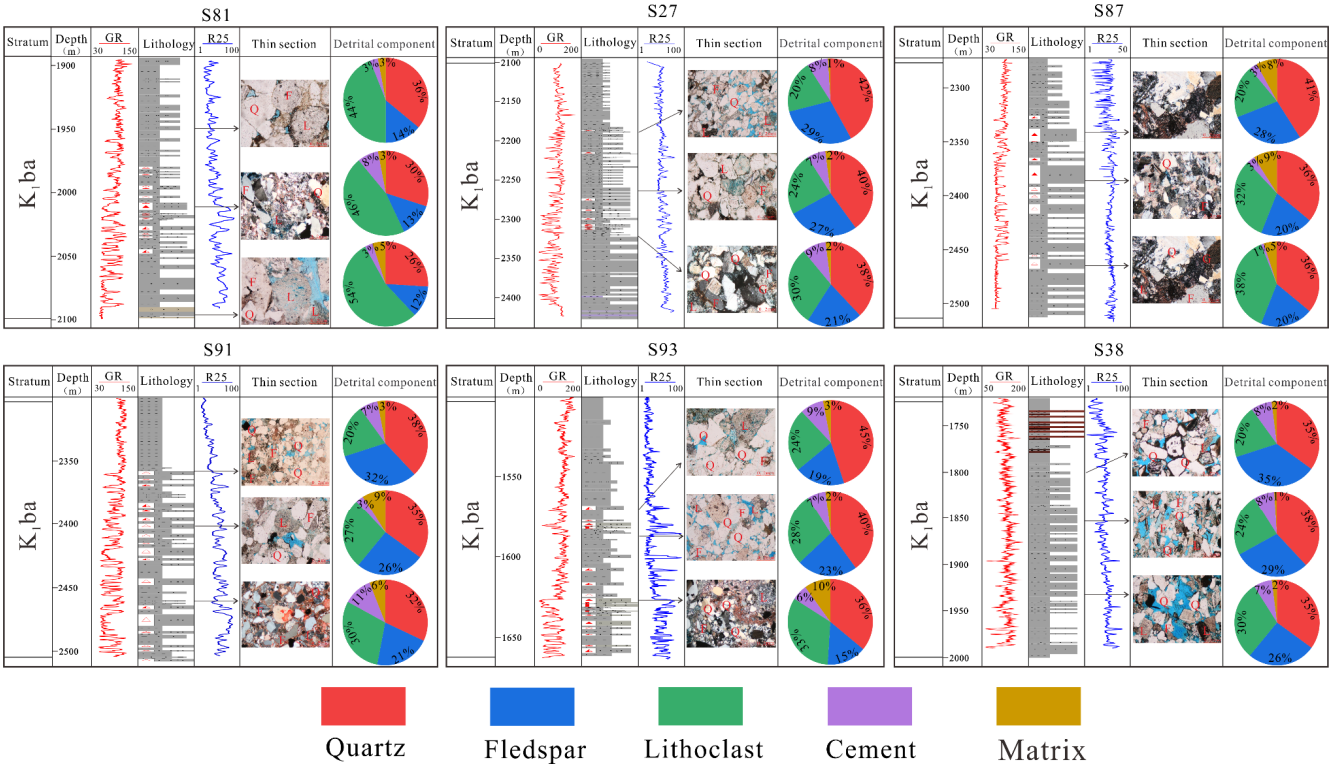

Figure 5. Characteristics of debrital components in A'ershan Formation in Saidong sub-sag, Saihantala sag. Abbreviations: Q: Quartz; F: Feldspar; L: Lithoclast; G: Granite.

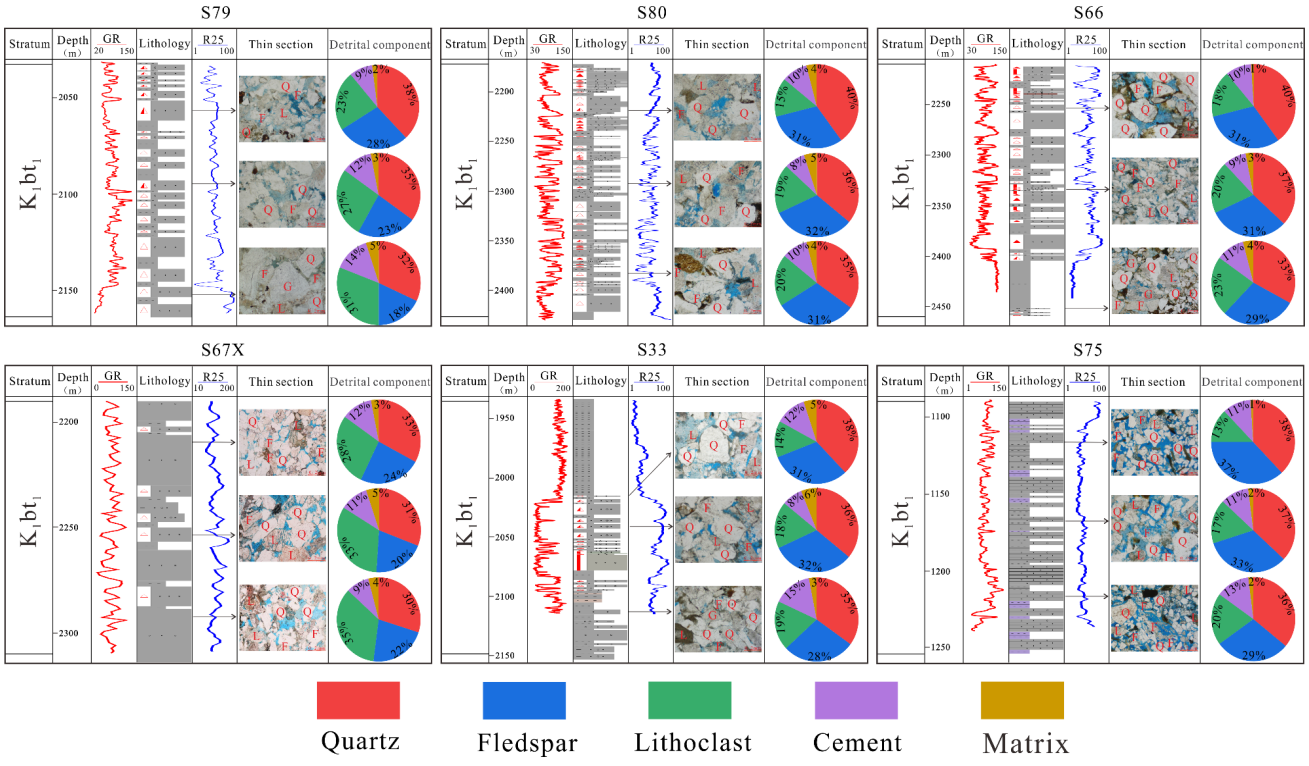

Figure 6. Characteristics of debrital components in member 1 of the Tengge'er Formation in Saidong sub-sag, Saihantala sag. Abbreviations: Q: Quartz; F: Feldspar; L: Lithoclast; G: Granite.

4.1.3. Grain Size Analysis

During the handling process, debris substances will change in mineral composition, particle size, sorting, and shape. The particle size of clastic rocks will change with different sedimentary environments, and the hydrodynamic force of a fan delta is caused by both gravity flow and traction flow [10,71–73]. Therefore, it is necessary to figure out particle size features to determine the hydrodynamic conditions and sedimentary environment of clastic sediments in the study area. An ideal probability cumulative grain size curve is mainly composed of three sub-populations, representing rolling, jumping, and suspension transport components. According to these three characteristics, 17 samples from 12 wells (Detailed data are shown in Supplementary Table S1) in the study area were researched and analyzed, which formed the main probability cumulative grain size curve of three types of fan delta. In summary, the grain size characteristic gives priority to type II.

1. Type I: single-stage (Supplementary Figure S3a) and multi-stage (Supplementary Figure S3b).

The components of each stage have no obvious differentiation, featuring coarse debris particles, wide distribution, poor sorting, and a linear or slightly convex arc shape. The suspended component accounts for about 70%, reflecting the settlement of the debris flow and strong hydrodynamics. The energy of vertical debris flow is small, the bottom is the bulk medium-fine conglomerate supported by matrix particles (Supplementary Figure S4a), which is in sudden contact with fine sediment, and the scour structure is extremely developed. The central part is the bulk medium-fine conglomerate supported by matrix particles (Supplementary Figure S4b), and the top is the bulk medium-fine sandstone-containing gravel. The mudstone drift gravel (Supplementary Figure S4c) and debris tearing and deformation structure are common in sandstone (Supplementary Figure S4d). This kind of curve is often found in the fan delta plain debris flow belt caused by gravity flow. The content of multi-stage coarse debris is high, which can reach 55% to 60%, and the content of gravel is between 10% and 25%, indicating the strong transport capacity of the water body. The coarse debris particles are mostly filled with medium to coarse sand, and the content of fine sand, silt, and clay is low. The analysis indicates that the upper part of the fluid is predominately transported by suspension and jumping, and the lower part of the fluid is mainly transported by rolling and elapsing, which represents a high-energy environment with poor sorting and rapid accumulation. Similar to debris flow caused by gravity flow, the lithology is mostly medium-fine sandstone with a massive structure (Supplementary Figure S4e) and medium-fine conglomerate supported by the matrix (Supplementary Figure S4f). This type of curve only appears in the braided river channel of the fan delta plain.

2. Type II: three-stage (Supplementary Figure S3c).

Rolling components are mostly composed of coarse sandstone with low content between 1% and 5%. The jumping component has a higher content ranging from 75% to 85%, with a coarse cut point between 0–1 φ and a fine cut point between 2–3 φ. Suspended components usually range from 5% to 10%. Transportation is dominated by traction flow, which indicates that the sedimentary environment has experienced strong hydrodynamic forces with a gradual weakening. After the fast-moving braided branch canals bring sediment into the lake, they are affected by the multi-direction and multi-group flow of the lake basin, constantly carrying sedimentary underwater diversion channel gravel, generally medium and fine sandstone, with a cross cushion or gravel layer (Supplementary Figure S4g).

3. Type III: two-stage (Supplementary Figure S3d).

This type can be subdivided into high-slope jumping and low-slope suspension. The jumping component content ranges from 60% to 70%, containing a small amount of medium sand, but mostly fine sand with moderate sorting and better grinding; the suspended component content ranges from 10% to 15%, containing mixed siltstone with poor sorting. It exhibits a reverse rhythmic sedimentary sequence and usually develops into small interlayers and horizontal stratigraphies of fine-grained sandstone or silty mudstone

(Supplementary Figure S4h). This is derived from the transportation of traction flow and lake waves, reflecting the far end of the fan delta front and the mudstone environment of prodelta transition to lacustrine facies.

4.1.4. Analysis of Sedimentary Facies Characteristics

1. Fan delta plain subfacies

The fan delta plain is mostly developed in an oxidation environment with strong hydrodynamic conditions and fast accumulation [74]. Four microfacies, namely braided channel, clastic flow zone, sheet flow zone, and inter-fan zone, can be identified in the Saidong sub-sag. On seismic profiles, the fan delta plain deposits typically present a wedge-type and chaotic progradational seismic reflection (Figure 7a). Generally, the logging curve is a box-bell-shaped combination (Supplementary Figure S5). Fan delta plain subfacies can be found in well S81, well S26, well S79, and well S90 in the study area. This paper takes well S81 as an example (Supplementary Figure S5) to study the sedimentary characteristics of fan delta plain subfacies and microfacies.

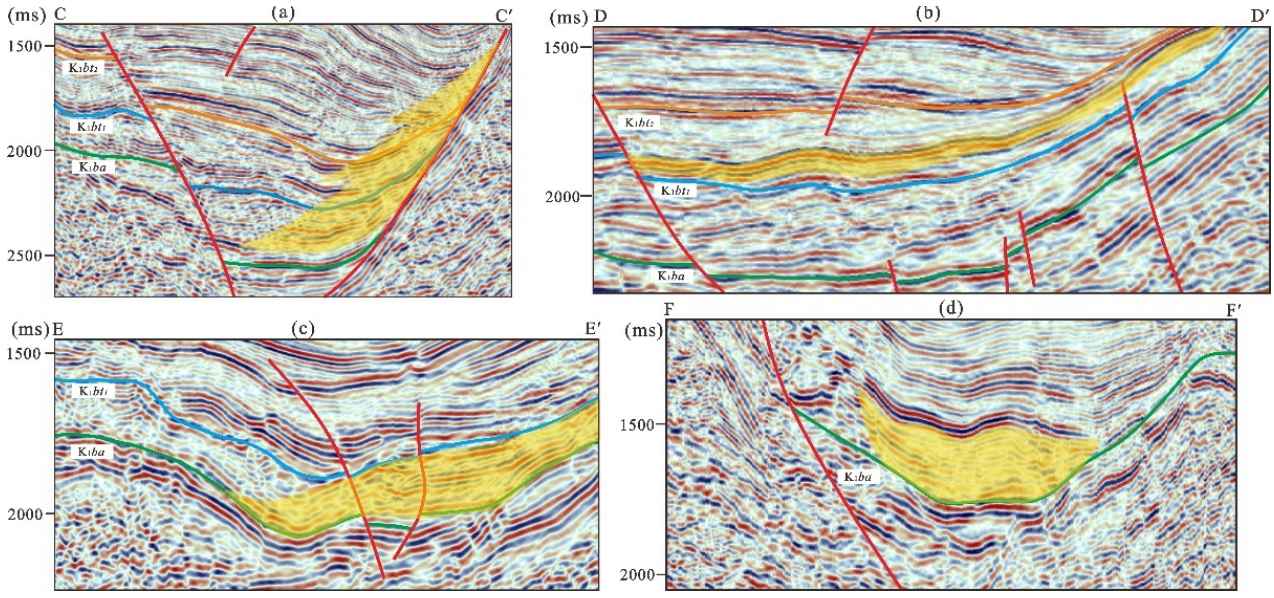

Figure 7. Seismic facies recognized in the Lower Cretaceous secession of the Saihantala sag. (**a**) Wedge-type and chaotic progradational seismic facies. (**b**) S-type progradational seismic facies. (**c**) Downlap-type progradational seismic facies. (**d**) Filled seismic facies. See Figure 1c for the location of these profiles. (The red line represents the faults. The green, blue and orange lines represent the tops of strata K_1ba, K_1bt_1 and K_1bt_2.).

(1) Braided river channel. It is the most developed microfacies in the fan delta plain subfacies and is usually formed in the late flood period [75,76]. A great number of clastic sediments are transported by debris flow and traction flow. The lithology is mainly composed of pebble conglomerate, with a small amount of arenaceous argillaceous sediments, poor gravel sorting and grinding, and higher content of the fine-silty matrix. Additionally, gravel is supported by the matrix and manifested by the micro-dentate box-shaped logging curve.

(2) Debris flow. It is formed by the accumulation of a great number of water bodies mixed with debris along the groove or sector surface of the sector in the early period of the flood [77]. The shape and distribution of debris flow are proportional to the hydrodynamic strength. When the hydrodynamic force is weak, the debris flow may be a band distribution along the groove, otherwise, it is a fan-shaped distribution [66]. The lithology of the debris flow features coarse clastic, mostly pebble conglomerate with arenaceous and argillaceous sediments whose sorting and rounding are poor,

most of which are sub-angular and angular, with high hybridity. Moreover, the debris particles are disorderly arranged, with a high content of the argillaceous and silty matrix, leading to poor reservoir capability. By and large, the overall responses of logging curves tend to be straight with high gamma and resistivity.

(3) Sheetflood zone. It is formed when the debris sediments were carried by floods which spilled over the braided river channel, due to the continuous erosion and transformation of the braided river channel. Its distribution is unstable and easily mixed with the sandbody of the braided river channel [75,76]. The lithology comprises pebble-granule conglomerate with argillaceous sediments, commonly observed through cross bedding, block bedding, parallel bedding, etc. On logging curves, the sheet flood zone deposits are featured by dentate-like box-shaped GR responses.

(4) Inter-fan belt. It is mainly distributed on both sides of the fan delta plain subfacies, formed by the deposition of fine debris carried by fan water flows (floodwater or fan rain) or wind [78], which is home to fine-grained clastics such as brown mudstone, silty mudstone, and silty-fine sandstone with small monolayer-thickness mudstone. On logging curves, the inter-fan belt deposits have slightly flat-straight GR responses.

The lithology of the lower part of the A'ershan Formation (K_1ba) in well S81 comprises glutenite intercalated with thick gray mudstone, and the upper part is fine-grained sandstone mixed with colored mudstone. Oil and gas occurred in the middle and lower A'ershan Formation. The SP responses (Supplementary Figure S5) indicate an obvious dentate-like box-bell-shaped combination. The hydrodynamic force is weak during sedimentation, where the coarse-grained clastic sediment distribution is far from orderly. The braided river channel microfacies are developed, leading to a clear vision of debris flow and inter-fan zone, as well as an occasional presence of the interchannel microfacies. From the end of the sedimentation of the A'ershan Formation to the beginning of the first member of the Tengge'er Formation (K_1bt_1), the whole area was in the water transgression. Hence, at the same time, the sediment grain size in the upper part of well S81 became thinner, resulting in a large number of the inter-fan zone and interchannel microfacies, and a sharp reduction of debris flow microfacies.

2. Fan delta front subfacies

As the subaqueous part of the fan delta [79], fan delta front deposits present a typical "S" progradational seismic reflection (Figure 7b), downlap-type progradational seismic facies (Figure 7c), or filled seismic reflection (Figure 7d). Compared with the fan delta plain, the grain size of the fan delta front is much finer, whose lithology is characterized by gray pebbled sandstone, mud-poor coarse- and fine-grained sandstone, and better grinding. Furthermore, four microfacies, including the subaqueous distributary channel, inter-distributary channel, mouth bar, and sand sheet, can be identified in the Saidong sub-sag (Supplementary Figure S7), which can be found in well S56, well S80, well S66, well S45, well S27, and well S69, and well S56 was chosen to investigate the sedimentary characteristics of fan delta front subfacies in the study area.

(1) Subaqueous distributary channel. It is the most developed microfacies of fan delta front subfacies, which is formed by the slump of the fan delta front sandbody in the steep slope, whose lithology is mostly gray pebbled sandstone and medium-grained sandstone with poor mudstone. Single-stage channel sand bodies were mostly in positive rhythms. From bottom to top, they often show normal grain order from pebble conglomerate to pebbled sandstone and sandstone, and composite rhythms are rarely found [67]. The scour surface usually appeared in the bottom with large cross bedding and parallel bedding, with bell-shaped or box-shaped responses in logging curves.

(2) Inter-distributary channel. It is mainly characterized by gray-green silty mudstone, argillaceous siltstone, and siltstone with small thickness layers. It has strong biological disturbance, thus conchostracan fossils and plant debris fossils can be found there [67].

The inter-distributary channel is responded to by a jagged GR response, which is formed by the underwater extension of the braided channel in the fan delta plain.

(3) Mouth bar. It is mainly developed at the estuary of the subaqueous distributary channel and is the accumulation of sand bodies after rushing out of the channel, usually extending to the center of the lake basin, with a relatively small deposition range and scale [80]. The lithology mostly comprises siltstone, argillaceous siltstone, and mudstone, showing the reverse rhythm of fine and coarse sandstone, with a high composition maturity and better sorting. Additionally, the wavy bedding is common to find, and the logging response is medium dentate funnel-shaped [81] (Supplementary Figure S7).

(4) Sand sheet. It is a fine-grained sand body with better sorting after being washed, sieved, and migrated by lake water [80], which is characterized by interbedded sandstone and mudstone, with thin and wide single layers. Thus, it resulted from weak hydrodynamic forces, and usually developed wavy bedding, with a dentate-shaped GR response (Supplementary Figure S7).

The main lithology of the second member of the Tengge'er Formation (K_1bt_2) in well S56 presented a conglomerate intercalated with thick mudstone. The color of the upper mudstone is mostly purple-red, while the lower becomes gray where oil and gas occurred. The SP curve showed a dentate-box shape, which indicated strong hydrodynamic forces and a sufficient supply of clastic sediments. During the sedimentation of the first member of the Tengge'er Formation (K_1bt_1), the water rapidly entered the whole area. In this period, fine-grained sediments, such as deep lacustrine mudstone or prodelta mud, and sand sheets microfacies were developed in well S56. During the sedimentation of the second member of the Tengge'er Formation (K_1bt_2), the whole area of the Saidong sag was dominated by a wide range of recessions, and the sedimentary lithology was mostly interbedded glutenite with gray calcareous mudstone, with a general development of distributary channel and inter-distributary channel microfacies, and yet rare sand sheet and mouth bar microfacies.

3. Prodelta subfacies

The prodelta was formed below the wave base, transiting to the deep lacustrine mudstone [82]. Its mud ratio was generally over 90%, with few lithologic interfaces. What is more, a thin layer of gray-black mudstone, silty mudstone, and horizontal bedding was developed [83]. The logging response is straight and stable, with high gamma and low resistivity. These subfacies could be found in well S27 and well S83X in the study area.

4.2. Sedimentary Facies Evolution and Their Planar Distributions

Based on the studies of lithology, sedimentary facies, and grain-size analysis in the study area, it is determined that there are three main stages during the deposition from the A'ershan Formation to the Tengge'er Formation in Saidong sub-sag, namely the water-transgression, the water oscillation, and the water regression [84], with distinct sedimentary planar distributions in each stage.

During the deposition of the A'ershan Formation (K_1ba) (Figure 8a), the eastern steep slope belt was the main source supply area [55], and the fan delta plain was developed in the eastern part of the trough near the source area, while the fan delta front crossed the whole trough from east to west. Due to the shallow water body and its limited range, the shore-shallow lake deposits were developed, pinching out from south to north. With the abundant source supply, the debris was transported for a long distance. Hence, large and independent fans with distant extensions were developed rapidly in a great number.

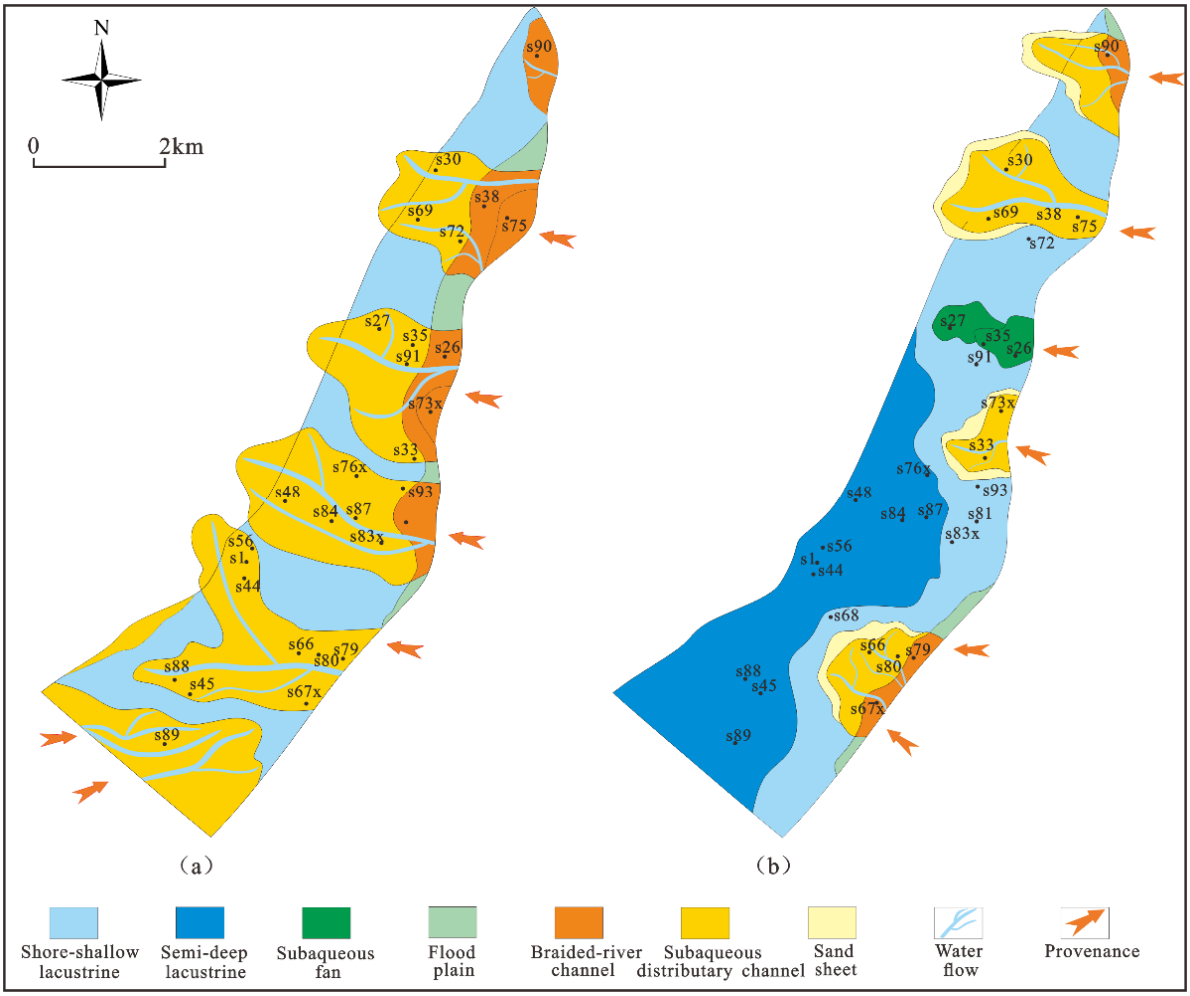

Figure 8. Planar distribution of sedimentary facies in Saidong sub-sag. (**a**) K_1ba sedimentary period and (**b**) K_1bt_1 sedimentary period.

During the deposition of Member 1 of the Tengge'er Formation (K_1bt_1) (Figure 8b), the lake basin was stably sunk, and the lake water invaded from the west to the east, resulting in a wide development of lacustrine deposits. A large set of semideep-deep lacustrine deposits were developed in the west and the southwest. Only a small range of fan delta front sediments and nearshore subaqueous fan deposits were developed in the eastern source area. The northern sand body was located at the hanging wall of the normal fault, as a result of sufficient source supplies. Therefore, fan delta sediments were developed.

During the V sand formation deposition of Member 2 in the Tengge'er Formation (Figure 9a), the lake basin was overall uplifted, followed a short period of recession, and then the rapid subsidence of the basin resulted in stable shallow water, leading to shore-shallow lake deposits. Several small fan bodies were formed successively in the eastern, northern, and southern areas. A small range of lacustrine fan was deposited near the deep lacustrine facies' deposition in the eastern provenance area. Nearshore subaqueous fan bodies were scattered on both sides of the north and south of the lake basin. A small range of braided river delta sedimentation was initially developed in the western gentle slope, thus the supply of clastic in the lake basin showed a multi-source trend.

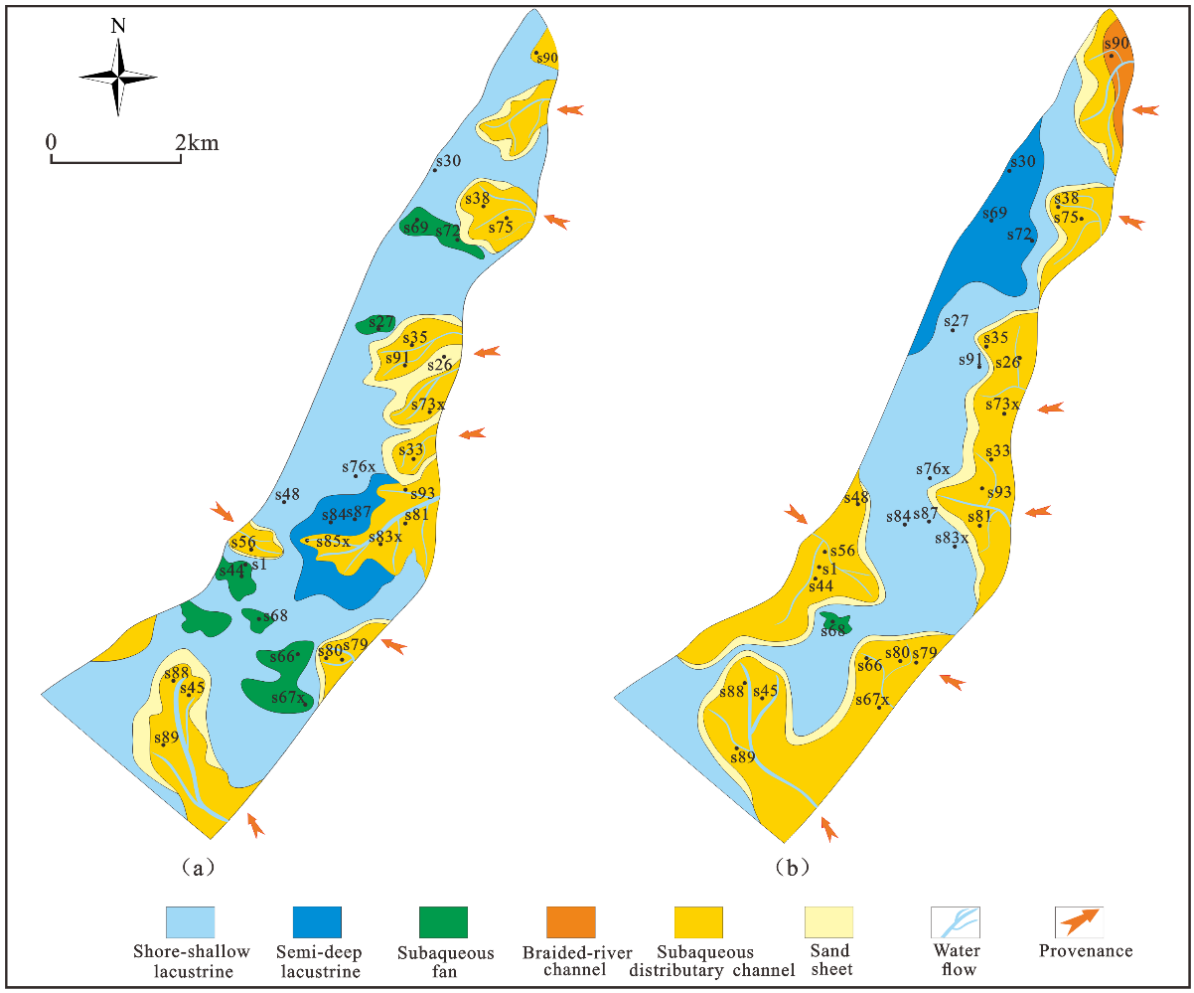

Figure 9. Planar distribution of sedimentary facies in Saidong sub-sag. (**a**) The V sand formation period of K_1bt_2 and (**b**) the IV sand formation period of K_1bt_2.

During the IV sand formation deposition of Member 2 in the Tengge'er Formation (Figure 9b), the lacustrine facies still played a major part. However, the source supply capacity on both sides was enhanced. The fan body had a larger distribution range and a longer extension distance compared with the former stage. The fan delta plain subfacies were mainly developed in the north, while the deep lacustrine sediments were shifted from the middle-east of the trough to the northwest, as a result of the continuous water regression.

During the III sand formation deposition of Member 2 in the Tengge'er Formation (Figure 10a), the water regression brought about the decreasing range of lacustrine facies and deep lacustrine facies. The fan delta continuously grew larger, and the provenance supply on the west side of the trough became greater, shown by the increase of the braided river delta in the west to the border with the southern and southeastern fan bodies.

During the II sand formation deposition of Member 2 in the Tengge'er Formation (Figure 10b), the deep lacustrine sediments disappeared, while the lacustrine deposits were merely found in the northwest of the trough, and sand bodies developed in the south. What is more, the abundant source supply came from the west and southeast sides of the trough.

During the I sand formation deposition of Member 2 in the Tengge'er Formation (Figure 10c), the sedimentary range of shore-shallow lacustrine in the northwest of the trough became larger and temporary water transgression occurred. The supply capacity of provenance in the southwestern depression gradually weakened, thus the range of fan bodies became smaller.

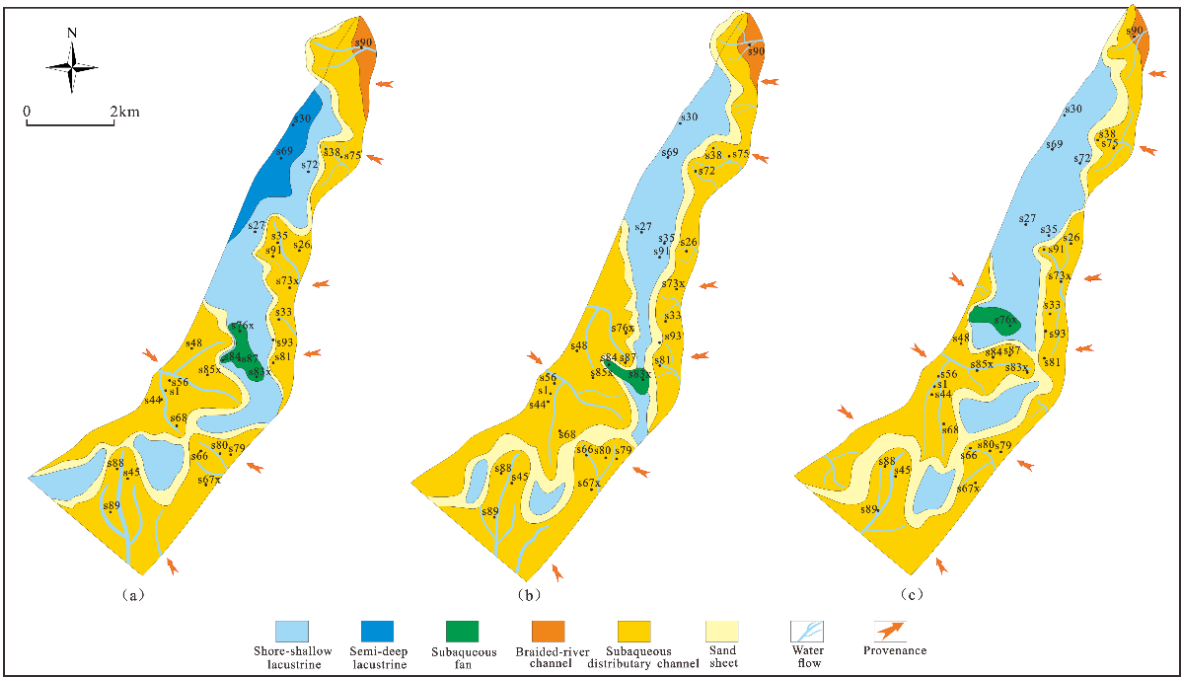

Figure 10. Planar distribution of sedimentary facies in Saidong sub-sag. (**a**) The III sand formation period of K_1bt_2, (**b**) the II sand formation period of K_1bt_2, and (**c**) the I sand formation period of K_1bt_2.

5. Discussion

Previous studies showed that the development of the sedimentary system is controlled by topographic slope, base-level cycles, material supply, paleoclimate, paleotectonic factors, and paleogeomorphology by different levels [9,10,52,53]. Based on the above studies, this paper suggests that the formation of the fan deltas in the study area was mainly controlled by paleotectonic factors and paleoclimate.

5.1. Paleoclimate

Lake level and provenance changes are controlled by paleoclimate, thus controlling the fan delta sedimentary characteristics and the evolution of sedimentary facies [85–87]. Generally, fan deltas can be developed both in a dry-hot and humid-hot environment. Under the dry-hot environment, landslides developed due to the lack of vegetation, thus causing the development of the fan delta of gravity flow genesis. Under the humid-hot environment, the vegetation plays an important role as the river flows in the fan delta stably flushed the existing sediments to form a fan delta dominated by traction flow. Due to limited data, we only discussed this controlling factor based on previous studies. The paleoclimate change and sedimentary facies have a significantly close relationship [88]. From the Upper Jurassic to the early Lower Cretaceous period, the sporo-pollen in fossil groups came from relatively developed heat- and drought-tolerant plants such as Classopollis, and then the Pinuspollenites gradually dominated. Under arid climatic conditions, underfilled lacustrine basins experienced lake-level falls caused by evaporation [27]. In the early Lower Cretaceous deposition, the previously formed isolated fan deltas continued their development. Controlled by stress relief, fan deltas had features of undeveloped delta plains and far-reaching delta front sand bodies [62,89]. From the early Lower to the middle Lower Cretaceous period, the number of the Densoisporites and Lygodiumsporites increased rapidly [90], which indicated that the region was controlled by the warm and humid climate complicated by paleoclimate fluctuations. It was speculated that the semi-deep to deep lacustrine facies were developed in this period, indicating that the area had been affected by lake waves. In this period, the lake expanded, whereas the fan deltas retrograded and the distribution areas of fan deltas decreased. Until the semi-arid climate period came in the late Lower Cretaceous period, the spore-pollen content of heat- or

drought-tolerant plants represented by Classopollis and Schizaeoisporites had achieved a significant peak, while the obvious decline in the content of the Pinuspollenites indicated the semi-arid climate period [91]. During this depositional period, the lake basin was characterized by a comparatively smaller extent, and large amounts of sediment were delivered from the western gentle slope belt into the lake and subsequently formed fan-shaped distributions. It is comprehensively analyzed that the paleoclimate change in the Saidong sub-sag experienced a semi-arid to hygrothermal to semi-arid trend, which is consistent with the development of fan deltas. The paleoclimatology fluctuation in the study area was basically consistent with the Lower Cretaceous area in the Songliao Basin, Northeast China [91].

5.1.1. Rock Color Differentiation

Based on the study of well S80 (Figure 11a), gray pebbled fine sandstone and brown-red argillaceous siltstone were mainly developed during the late period of K_1ba to the early period of K_1bt_1, which indicated the arid environment of the sediments. The occurrence of a thick layer of black carbonaceous mudstone and a coal seam in the K_1bt_1 indicated that the study area had experienced a humid environment during this stage (Figure 11b), which was also consistent with the regional transgression background. During the sedimentary period of the member III sand group of K_1bt_2, the development of varicolored glutenite and gray-white mudstone (Figure 11c) indicated the water turbulence during this stage and the semi-humid to semi-arid paleoclimate. The core of the member I sand group of K_1bt_2 was mainly composed of purple to purple-red mudstone and varicolored glutenite, which represents the arid environment during the deposition of this member (Figure 11d).

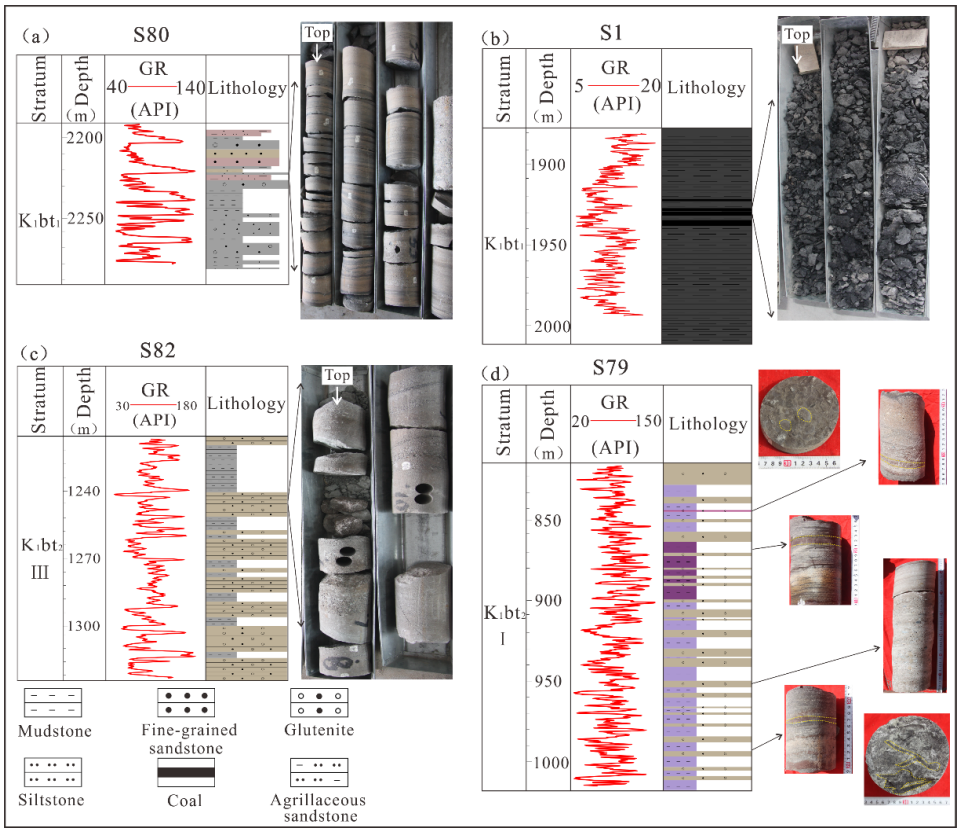

Figure 11. Lithological characteristics of the study area in different sedimentary periods. (**a**) well S80, gray pebbled fine sandstone and brown-red argillaceous siltstone, (**b**) well S1, thick layer of black carbonaceous mudstone and a coal seam, conchostracan fossils with fewer plant debris fossils (**c**) well S82, varicolored glutenite and gray-white mudstone, (**d**) well S79, purple to purple-red mudstone and varicolored glutenite, plant debris fossils.

In summary, the sediments from the Lower Cretaceous period in the study area alternately exhibited dark-gray to gray glutenite, varicolored glutenite with purple to purple-red mudstone, or argillaceous siltstone from bottom to top, reflecting the alternate evolution characteristics of the sedimentary environment from aquatic oxidation to a subaqueous reduction environment.

5.1.2. Fossils

In addition to the change of rock color, fossils' differences can also be used as an index of the paleoclimate changes [10,87]. The occurrence of numerous plant debris fossils in the K_1ba indicated the semi-oxidative environment of a humid climate during this period [92]. During the deposition of K_1bt_1, the appearance of conchostracan fossils (Figure 11b) with fewer plant debris fossils indicated a warm and humid deacidizing environment. During the deposition of the K_1bt_2, the decrease in conchostracan fossils and increase in plant debris fossils indicated that the paleoclimate gradually transited from semi-humid to semi-arid during this period. The paleoclimate change from semi-arid to hygrothermal to semi-arid showed that the basin was probably gradually uplifted.

5.2. Tectonic Constraints

The Erlian Basin is a Mesozoic–Cenozoic lacustrine rift basin developed on a Palaeozoic folded basement resulting from a large-scale soft collision [62,93,94]. The paleogeomorphology was thought to be dominantly controlled by the evolution of regional faults, thus showing the influences on the sedimentary system and depositional pattern [95]. During the early Cretaceous period, the activation of the Xilin fault and the Zhabu fault formed a half-graben structure with a fault depression on the west and overlaps on the east in the Saidong sub-sag, but there was a slight difference among the stages of different members. During the stage of K_1ba (Figure 12a,b and Figure 13a), the extension of the sag was about 0.48 km and the elongation was 1.77% (calculated after Figure 3). The Saidong sub-sag mainly developed fan delta deposits. During the stage of K_1bt_1 (Figures 12c and 13b), the extension of the sag was about 0.09 km and the elongation was 0.32% (calculated after Figure 3). The study area experienced an actively extensional rifting period, and the eastern steep zone developed nearshore subaqueous fan deposits on the existing early fan delta, and the western part developed fan delta sediments. Under the background of large-scale water transgression, the subsidence rate of the basin was greater than the deposition rate, therefore, the semi-deep lacustrine facies was developed as well. During the stage of K_1bt_2 (Figures 12d and 13c), the deposition rate was greater than the subsidence rate due to the weakened activity of the Zhabu fault, causing the rapid deposition of clastic sediments from the margin to the center of the lake basin, which eventually formed a great number of fans. The extension of the sag was about 1.1 km and the elongation came to 4% (calculated after Figure 3). During the stage of K_1bs (Figure 13d), the extension of the sag added up to about 0.64 km and the elongation came to 2.23% (calculated after Figure 3). The fault activity was nearly ceased; therefore, the lake basin began to vanish, while fluvial facies started to develop. The activation of the two major faults controlled the filling model of the Saidong sub-sag and the distribution of the fan deltas in the study area as well. The tectonic evolution of this region controlled the evolution of the lake basin in the Saihantala sag and further controlled its depositional systems' distribution, especially the connection and retrogradation of the braided delta and fan delta deposits and the appearance of the nearshore subaqueous fan deposits. The Saidong sub-sag belt mainly experienced an early-middle activated single-cycle faulting pattern, which exerted a controlling effect on the development and distribution of the fan delta deposits [62].

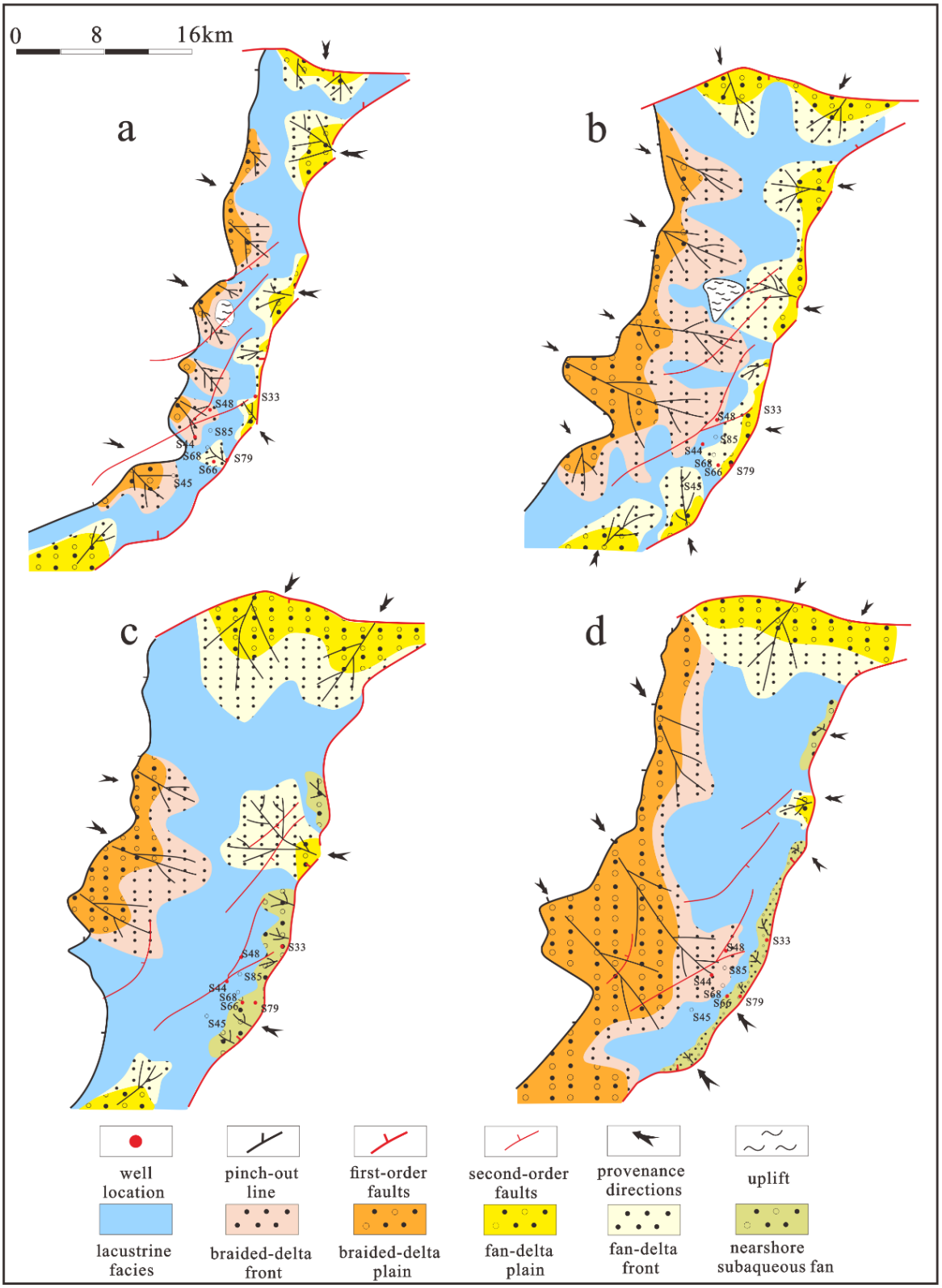

Figure 12. Planar distribution of depositional systems in the Lower Cretaceous Saihantala sag [62,63] indicating sedimentary facies evolution of the sag. (**a**) Planar distribution of depositional systems in the Saihantala sag during the depositing period of LK_1ba. (**b**) Planar distribution of depositional systems in the Saihantala sag during the depositing period of UK_1ba. (**c**) Planar distribution of depositional systems in the Saihantala sag during the depositing period of K_1bt_1. (**d**) Planar distribution of depositional systems in the Saihantala sag during the depositing period of K_1bt_2.

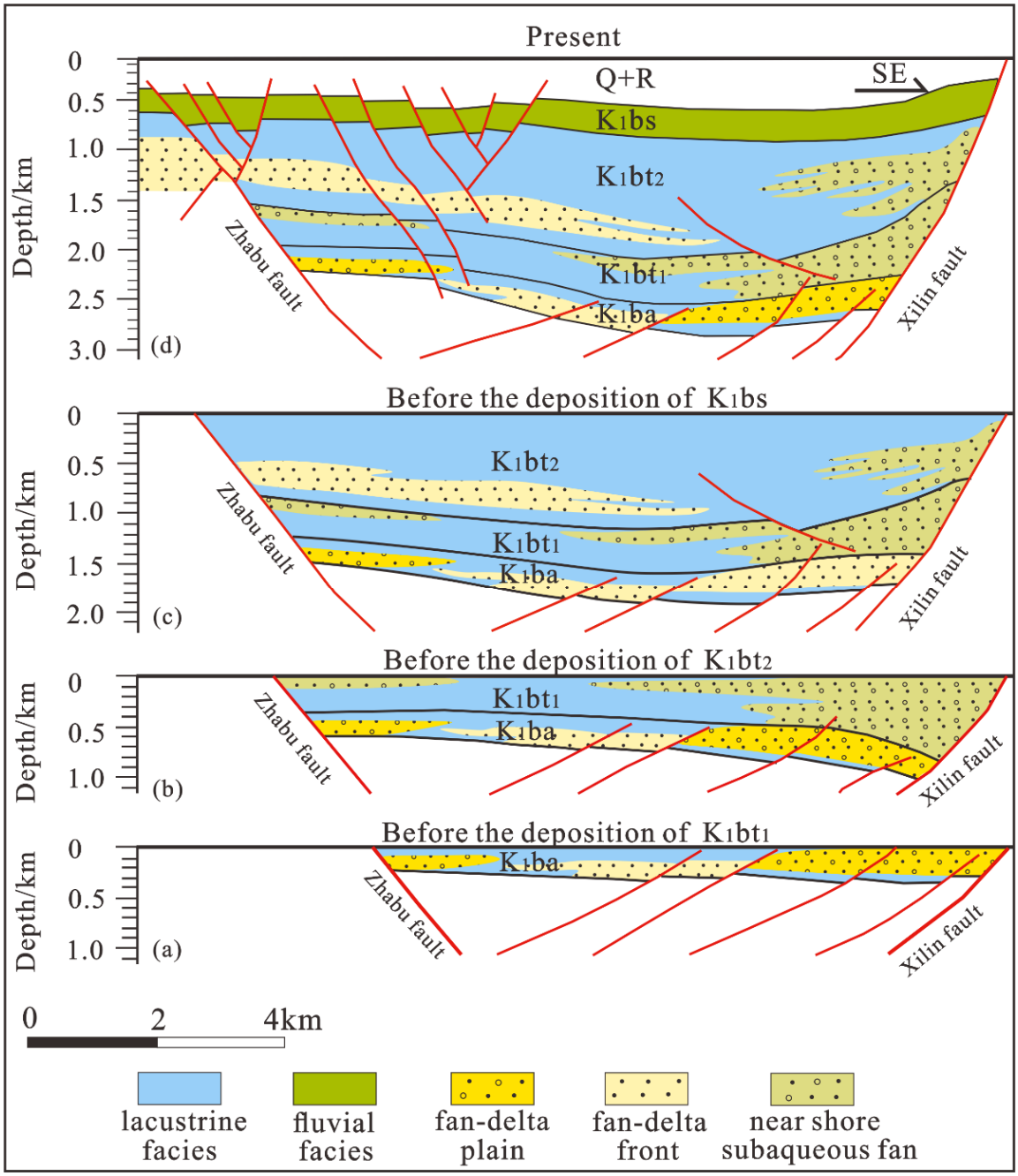

Figure 13. Deposition pattern of the Saidong sub-sag controlled by tectonic faults [62]. (**a**) Deposition pattern of the Saidong sub-sag during the depositing period of K_1ba. (**b**) Deposition pattern of the Saidong sub-sag during the depositing period of K_1bt_1. (**c**) Deposition pattern of the Saidong sub-sag during the depositing period of K_1bt_2. (**d**) Deposition pattern of the Saidong sub-sag during the depositing period of K_1bt_1 at present. (The red line represents the faults).

5.3. Sedimentary Model

Based on the analysis of sedimentary controlling factors, the sedimentary model of the fan deltas in the study area was established (Figure 14). In the semi-arid climate environment, the relatively slow transportation of debris formed small and independent fans. In the warm and humid climatope, debris can be transported from the valley by strong hydrodynamic force which accumulated at the foot of the mountain and formed a fan delta plain. Detrital flow deposits were formed at the foot of the mountains during the flooding period, while sheet flow was mainly formed in plains. Braided river channels were

often developed in existing river trenches during the middle-late flooding periods. Detrital sediments carried by the river entered the lake basin through the braided channel, forming subaqueous distributary channel deposits at the fan delta front. The dominant traction flow during this period caused great extension of the river, thus screening the detrital sediments and forming gravel sand bodies. The wave of the lake and the coastal water action constantly washed and screened the sand bodies of the subaqueous distributary channel, eventually forming fine-grained sheet sand sediments in front of the river mouth bar. Under the hydrostatic condition of the semi-deep lake-deep lake, the argillaceous sediment in the sand body was slowly deposited, forming a deep lake facies dark mudstone without an obvious boundary.

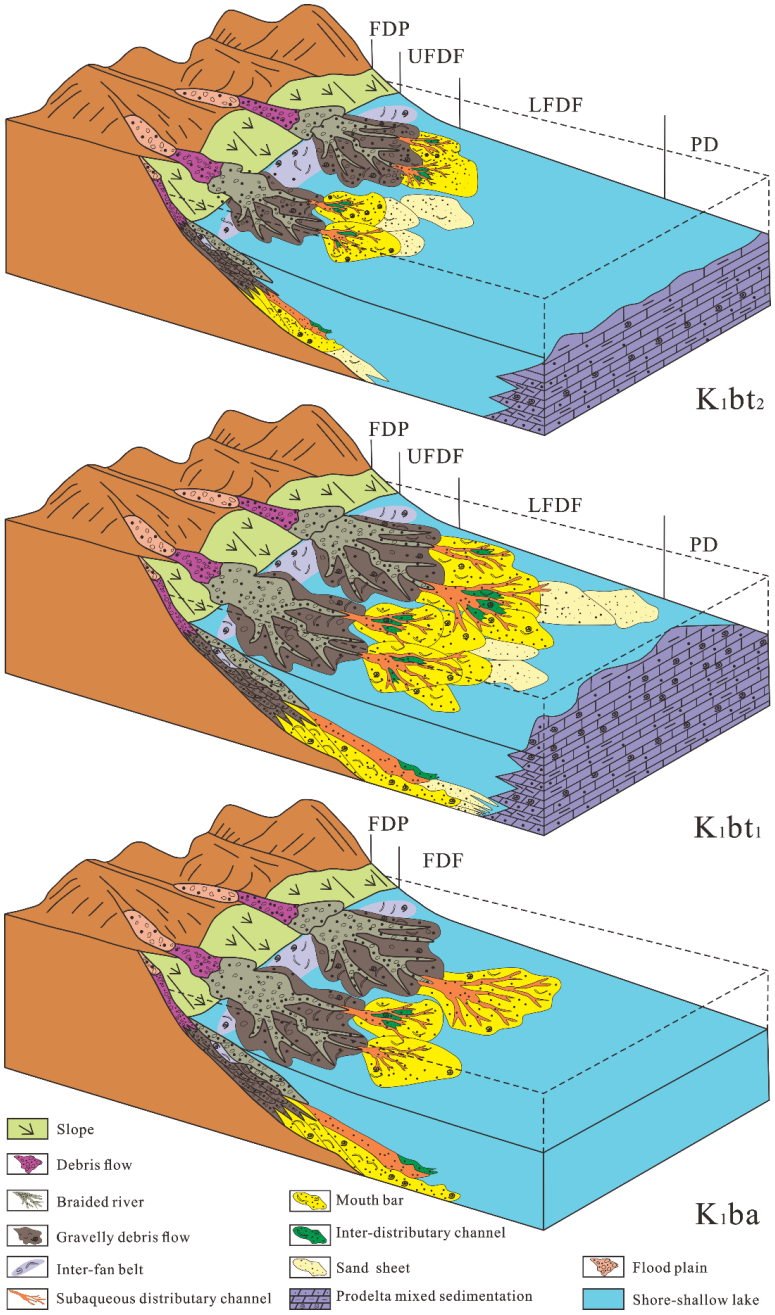

Figure 14. Sedimentary facies types and models of fan delta in Saidong sub-sag, not to scale. Abbreviations: FDP, fan delta plain; UFDF, upper fan delta front; LFDF, lower fan delta front; PD, prodelta.

6. Conclusions

By employing core observations from 28 newly drilled wells, as well as the particle size analysis, well logging, and seismic interpretation, the current work has propelled insights into lithologic characteristics, sedimentary facies characteristics, sedimentary facies evolution and their planar distribution, and the paleoclimate and paleostructure of the Lower Cretaceous fan deltas in Saidong sag, Saihantala sag, Erlian Basin, in order to determine the sedimentary characteristics and the main controlling factors of the Lower Cretaceous fan deltas in the Saidong sub-sag. Major conclusions derived from this research are:

(1) The Lower Cretaceous fan deltas in the Saidong sub-sag can be divided into 3 categories, 12 sub-categories, and 20 fine lithofacies types. From the lithofacies characteristics, genetic mechanism, and distribution of different lithofacies, the proportion of fan delta traction flow in the study area is higher than gravity flow.

(2) The Lower Cretaceous fan deltas in the Saidong sub-sag of the Saihantala sag mainly developed three subfacies, namely fan delta plain, fan delta front, and prodelta, and can be further subdivided into eight microfacies, including braided river channel, subaqueous distributary channel, inter-distributary channel, mouth bar, and sand sheet, with the braided river channels and subaqueous distributary channels as the major microfacies. Based on the vertical evolution of the sedimentary and lithofacies characteristics of each microfacies at the sand body, we believe that the A'ershan Formation to Tengge'er Formation in the Saidong sub-sag mainly experienced three stages: the water transgression period, the water oscillation period, and the water regression period. Each stage has different sedimentary evolution features.

(3) The fan delta deposits in the Saidong sub-sag are mainly controlled by a semi-arid to hygrothermal to semi-arid paleoclimate as well as paleotectonic activity. The fan delta sedimentary pattern of the Saidong sub-sag in the Saihantala sag established in this study can improve the differentiation and classification of the fan delta sedimentary characteristics in other potential areas of the Erlian Basin.

Supplementary Materials: The following supporting information can be downloaded at: https://www.mdpi.com/article/10.3390/en15228373/s1, Figure S1: Section AA' of Saidong Sub-Sag in Saihantala Sag, Erlian Basin; Figure S2: Section BB' of Saidong Sub-Sag in Saihantala Sag, Erlian Basin; Figure S3: Probability cumulative grain-size curve of the study area, Figure S4: Typical core photos of sedimentary structure in Saidong Sub Sag, Figure S5: Morphological characteristics of typical logging curves in fan delta plain facies, Figure S6: Fan delta plain facies model (Well S81), Figure S7: Fan delta front facies model (Well S56), Table S1: Detailed data in Figure S3.

Author Contributions: Conceptualization, B.Y., H.Y. and X.S.; methodology, B.Y.; software, B.Y.; validation, B.Y., H.Y. and T.Z.; formal analysis, B.Y.; investigation, B.Y.; resources, H.Y.; data curation, S.L.; writing—original draft preparation, B.Y.; writing—review and editing, B.Y. and H.Y.; visualization, B.Y. and T.Z.; supervision, H.Y.; project administration, H.Y.; funding acquisition, H.Y. All authors have read and agreed to the published version of the manuscript.

Funding: This research was funded by Ministry of Education Industry-University Cooperation Education Project, grant number 2019023020045. This work was also supported by National Natural Science Foundation Project (41572126) and Central Support Project for Young Talents in Local Universities in Heilongjiang Province (14011202101).

Institutional Review Board Statement: Not applicable.

Informed Consent Statement: Not applicable.

Data Availability Statement: The data used to support the findings of this study are included within the article.

Acknowledgments: Thanks to Huabei Oilfield Branch of Petro-China for basic data in this project. We are also very grateful to the reviewers and editors for their contributions to improving this paper.

Conflicts of Interest: The authors declare that they have no conflict of interest.

References

1. Colella, A. Fault-controlled marine Gilbert-type fan deltas. *Geology* **1988**, *16*, 1031–1034. [CrossRef]
2. Postma, G.; Colella, A.; David, B.P. Depositional architecture and facies of river and fan deltas: A synthesis. *Coarse Grained Deltas* **1990**, *10*, 13–27.
3. Gupta, S.; Underhill, J.R.; Sharp, I.R.; Gawthorpe, R.L. Role of fault interactions in controlling synrift sediment dispersal patterns: Miocene, Abu Alaqa Group, Suez Rift, Sinai, Egypt. *Basin Res.* **1999**, *11*, 167–189.
4. Breda, A.; Mellere, D.; Massari, F.; Asioli, A. Vertically stacked Gilbert-type deltas of Ventimiglia (NW Italy): The Pliocene record of an overfilled Messinian incised valley. *Sediment. Geol.* **2009**, *219*, 58–76. [CrossRef]
5. Gobo, K.; Ghinassi, M.; Nemec, W. Reciprocal changes in foreset to bottomset facies in a Gilbert-type delta: Response to short-term changes in base level. *J. Sediment. Res.* **2014**, *84*, 1079–1095. [CrossRef]
6. Gobo, K.; Ghinassi, M.; Nemec, W.; Sjursen, E. Development of an incised valley-fill at an evolving rift margin: Pleistocene eustasy and tectonics on the southern side of the Gulf of Corinth, Greece. *Sedimentology* **2014**, *61*, 1086–1119. [CrossRef]
7. Gobo, K.; Ghinassi, M.; Nemec, W.; Walsh, J.P. Gilbert-type deltas recording short-term base-level changes: Delta-brink morphodynamics and related foreset facies. *Sedimentology* **2015**, *62*, 1923–1949. [CrossRef]
8. Martini, I.; Ambrosetti, E.; Sandrelli, F. The role of sediment supply in large-scale stratigraphic architecture of ancient Gilbert-type deltas (Pliocene Siena-Radicofani Basin, Italy). *Sediment. Geol.* **2017**, *350*, 23–41.
9. Yu, H.T.; Liu, X.Y.; Wu, B.W.; Liu, X.M. Large Fan Delta Control Factors of Upper Wuerhe Formation of Shawan Sag in Northwest Margin of Junggar Basin. *Xinjiang Geol.* **2020**, *38*, 71–76.
10. Zhang, C.; Yu, X.H.; Yao, Z.Q.; Li, L.S.; Shan, X.; Xiang, M.; Li, Y.L. Sedimentary evolution and controlling factors of the Middle-Upper Jurassic in the western part of the southern Junggar Basin. *Geol. China* **2021**, *1*, 284–296.
11. Yue, J.H.; Huang, C.Y.; Cao, L.Z.; Wang, H.X.; Zheng, R.H.; Wu, J.P.; Xiang, X.; Liu, H. Sedimentary characteristics and controlling factors of the Ba 66 Fan in Bayindulan Sag. *Bull. Geol. Sci. Technol.* **2021**, *40*, 88–98.
12. Winsemann, J.; Lang, J.; Polom, U.; Loewer, M.; Igel, J.; Pollok, L.; Brandes, C. Ice-marginal forced regressive deltas in glacial lake basins: Geomorphology, facies variability and large-scale depositional architecture. *Boreas* **2018**, *47*, 973–1002. [CrossRef]
13. Winsemann, J.; Lang, J.; Fedele, J.J.; Zavala, C.; Hoyal, D.C.J.D. Re-examining models of shallow-water deltas: Insights from tank experiments and field examples. *Sediment. Geol.* **2021**, *421*, 105962. [CrossRef]
14. Zhao, G.L.; Zhao, C.L.; Ye, L.J. Sedimentary System of "Four Fans and One Channel" In the Bohai Gulf Basin and Its Significance for Petroleum Exploration. *J. Geomech.* **2005**, *3*, 245–258.
15. Liang, H.B.; Cui, Z.Q.; Dong, X.Y.; Li, H.E.; Si, J.W.; Wang, Y.J. Characteristics of Highstand Delta System and Play in Gentle Slop of Faulted Lacustrine Basin: A Case Study of Jiergalangtu Sag, Erlian Basin. *Acta Sedimentol. Sin.* **2011**, *29*, 783–792.
16. Liang, G.Z.; Tan, J.C.; Wei, L.; Jiang, Y.; Cao, W.; Wu, W.L.; Guo, X.G. Sedimentary characteristics of nearshore subaqueous fans of the Lower Cretaceous in Abei sag of Erlian Basin, Inner Mongolia. *J. Palaeogeogr.* **2013**, *15*, 31–42.
17. Song, G.Q.; Hao, X.F.; Liu, K.Q. Tectonic evolution, sedimentary system and petroleum distribution patterns in dustpan-shaped rift basin: A case study from Jiyang Depression, Bohai Bay Basin. *Oil Gas Geol.* **2014**, *35*, 303–310.
18. Gawthorpe, R.L.; Leeder, M.R. Tectono-sedimentary evolution of active extensional basins. *Basin Res.* **2000**, *12*, 195–218. [CrossRef]
19. Kim, W.; Paola, C. Long-period cyclic sedimentation with constant tectonic forcing in an experimental relay ramp. *Geology* **2007**, *35*, 331–334. [CrossRef]
20. Yu, X.H.; Jiang, H.; Li, S.L.; Chen, Y.Q. Depositional filling models and controlling factors on Mesozoic and Cenozic fault basins of terrestrial facies in eastern China: A case study of Dongying Sag of Jiyang Depression. *Lithol. Reserv.* **2007**, *19*, 39–45.
21. Henstra, G.A.; Gawthorpe, R.L.; Helland-Hansen, W.; Ravnås, R.; Rotevatn, A. Depositional systems in multiphase rifts: Seismic case study from the Lofoten margin, Norway. *Basin Res.* **2017**, *29*, 447–469. [CrossRef]
22. Shanley, K.W.; McCabe, P.J. Perspectives on the sequence stratigraphy of Continental strata. *AAPG Bull.* **1994**, *78*, 544–568.
23. Jackson, C.A.L.; Gawthorpe, R.L.; Carr, I.D.; Sharp, I.R. Normal faulting as a control on the stratigraphic development of shallow marine syn-rift sequences: The Nukhul and Lower Rudeis Formations, Hammam Faraun fault block, Suez Rift, Egypt. *Sedimentology* **2005**, *52*, 313–338. [CrossRef]
24. Hsiao, L.-Y.; Graham, S.A.; Tilander, N. Stratigraphy and sedimentation in a rift basin modified by synchronous strike-slip deformation: Southern Xialiao basin, Bohai, offshore China. *Basin Res.* **2010**, *22*, 61–78. [CrossRef]
25. Jiang, S.; Henriksen, S.; Wang, H.; Lu, Y.C.; Ren, J.Y.; Cai, D.S.; Feng, Y.L.; Weimer, P. Sequence-stratigraphic architecture and sand-body distribution in Cenozoic rifted lacustrine basins, east China. *AAPG Bull.* **2013**, *97*, 1447–1475. [CrossRef]
26. Jia, Y.C.; Lin, C.S.; Eriksson, K.A.; Niu, C.M.; Li, H.Y.; Zhang, P. Fault control on depositional systems and sequence stratigraphic architecture in a multiphase, rifted, lacustrine basin: A case study from the paleogene of the central Bohai Bay Basin, northeast China. *Mar. Pet. Geol.* **2018**, *101*, 459–475. [CrossRef]
27. Carroll, A.R.; Bohacs, K.M. Stratigraphic classification of ancient lakes: Balancing tectonic and climatic controls. *Geology* **1999**, *27*, 99–102. [CrossRef]
28. Lin, C.S.; Kenneth, E.; Li, S.T. Sequence architecture, depositional systems, and controls on development of lacustrine basin fills in part of the Erlian basin, northeast China. *AAPG Bull.* **2001**, *55*, 2017–2043.
29. Wu, C.Y.; Xue, S.H. *Sedimentology of Petroliferous Basins in China*; Petroleum Industry Press: Beijing, China, 1993; pp. 38–42.
30. Xie, X.N.; Sun, Y.C.; Deng, X.H.; Ding, Z.Y.; Han, G.L. Patterns of fan delta sequence and their controlled parameters. *Earth Sci.* **1993**, *6*, 749–756.

31. Xue, L.Q.; Galloway, W.E. Fan-Delta, Braid Delta And The Classification Of Delta Systems. *Acta Geol. Sin.* **1991**, *65*, 141–153.
32. Gómez-Paccard, M.; López-Blanco, M.; Costa, E.; Garcés, M.; Beamud, E.; Larrasoaña, J.C. Tectonic and climatic controls on the sequential arrangement of an alluvial fan/fan-delta complex (Montserrat, Eocene, Ebro Basin, NE Spain). *Basin Res.* **2012**, *24*, 437–455. [CrossRef]
33. Li, Y.X. Early Oligocene fan-deltas in Liaohe rift. *Pet. Explor. Dev.* **1982**, *4*, 21–27.
34. Gu, J.Y. Sedimientation of ancient fan-deltas in eastern China. *Oil Gas Geol.* **1984**, *3*, 236–245.
35. Nemec, W.; Steel, R.J.; Yao, G.Q. Fan Delta and Its Identification. *J. Gems Gemmol.* **1999**, *1*, 40–47.
36. Wang, H.J.; Cao, W.F. Lacustrine-deltaic deposits of Cretaceous in Song Liao basin. *Pet. Geol. Oilfield Dev. Daqing* **1983**, *2*, 15–24.
37. Einar, A.; Roy, H.G.; Eduardo, R. The significance of the fracture pattern of the Late-Eocene Montserrat fan-delta, Catalan Coastal Ranges (NE Spain). *Tectonophysics* **1996**, *266*, 465–491.
38. Mu, L.X.; Jia, A.L. *Reservoir Models and Prediction Method for Fan-delta*; Petroleum Industry Press: Beijing, China, 2000; pp. 19–91.
39. Wang, S.Q. Sedimentary facies and model of Shuanghe fan delta. *Xinjiang Pet. Geol.* **1986**, *3*, 26–34.
40. Sohn, Y.K. Coarse-grained debris-bow deposits in the Miocene fan-deltas, SE Korea: A scaling analysis. *Sediment. Geol.* **2000**, *130*, 45–64. [CrossRef]
41. Richard, G.H.; Kenneth, D.R. Sedimentology and sequence stratigraphy of fan-delta and river-deltadeposystems, Pennsylvanian Minturn Formation, Colorado. *AAPG Bull.* **2003**, *87*, 1169–1191.
42. McConnico, T.S.; Bassett, K.N. Gravelly Gilbert-type fan delta on the Conway Coast, New Zealand: Foreset depositional processes clast imbrication. *Sediment. Geol.* **2007**, *198*, 147–166. [CrossRef]
43. Yu, X.H.; Qu, J.H.; Tan, C.P.; Zhang, L.; Li, X.L.; Gao, Z.P. Conglomerate Lithofacies and Origin Models of Fan Deltas of Baikouquan Formation in Mahu Sag, Junggar Basin. *Xinjiang Pet. Geol.* **2014**, *35*, 619–627.
44. Wang, X.J.; Li, W.F.; Dong, H.; Zhu, J.; Zhang, D.Y.; Yin, S.J. Genetic Classification of Sandy Conglomerate lithofacies and Sedimentary Characteristics of Fan Delta: A Case Study from Upper Wuerhe Formation in District Wuba in Northwestern Margin of Junggar Basin. *Xinjiang Pet. Geol.* **2017**, *5*, 537–543.
45. Zhang, J.L.; Wang, B.Q. Facies Models For Lacustrine Fan Deltas In Hydrocarbon-Bearing Basins, China. *Geol. Rev.* **1996**, *42*, 147–152.
46. Zhang, C.S.; Liu, Z.B.; Shi, D.; Jia, A.L. Formed Proceeding and Evolution Disciplinarian of Fan Delta. *Acta Geol. Sin.* **2000**, *18*, 521–525.
47. Cheng, L.H.; Chen, S.Y.; Wu, S.H.; Yan, J.H.; Jiang, Z.X.; Wang, J.W.; Liu, Y.L. The Simulation And Sedimentary Dynamic Analysis Of Fan Delta In The Steep Slope Of Fault Basin. *Mar. Geol. Quat. Geol.* **2005**, *25*, 29–34.
48. Pang, J.G.; Yang, Y.Y.; Pu, X.G. Identification characteristics of fan delta, nearshore submarine fan, and sublacustrine fan in fault trough lake basin. *J. Lanzhou Univ. (Nat. Sci.)* **2011**, *47*, 18–23.
49. Ji, Y.L.; Lu, H.; Liu, Y.R. Sedimentary model of shallow water delta and beach bar in the Member 1 of Paleogene Funing Formation in Gaoyou sag, Subei Basin. *J. Palaeogeogr.* **2013**, *15*, 729–740.
50. Cheng, G.; Si, C.S.; Zhang, H.L.; Yan, X.F.; Liu, Y.F. Study on sedimentary numerical simulation method of fan delta sand body. *J. Geol.* **2013**, *37*, 178–182.
51. Zou, Z.W.; Li, H.; Xu, Y.; Yu, C.F.; Meng, X.C. Sedimentary characteristics of the Baikouquan Formation, Lower Triassic in Mahu Depression, Junggar Basin. *Bull. Geol. Sci. Technol.* **2015**, *34*, 20–26.
52. Jiang, Q.P.; Kong, C.X.; Li, W.F.; Qiu, Z.G.; Lu, Z.Y.; Hang, T.Q.; Liu, K.; Chen, D.L.; Li, S.; Yuan, X.G. Sedimentary Characteristics and Evolution Law of a Lacustrine Large-scale Fan Delta: A case study from the Triassic Baikouquan Formation on the west slope of Mahu Sag. *Acta Sedimentol. Sin.* **2020**, *38*, 923–932.
53. Zou, Z.W.; Guo, H.J.; Niu, Z.J.; Xu, Y.; Shan, X.; Li, Y.Z.; Shen, J.L. Sedimentary characteristics and controlling factors of river-dominated fan delta: A case study from Upper Urho Formation in Mahu Sag of Junggar Basin. *J. Palaeogeogr.* **2021**, *23*, 756–770.
54. Zhang, W.C. Sedimentary Feature of Fan Delta in Erlian Basin. *Fault-Block Oil Gas Field* **1998**, *5*, 3–5.
55. Cheng, Y.Q. Sedimentary characteristics study on Lower Cretaceous of Saihantala Sag, Erlian Basin. Master's Thesis, China University of Geosciences, Beijing, China, 2010.
56. Zhou, T.Q. Research on the Sedimentary Characteristics of the Glutenite in Lower Cretaceous of the Eastern Sag, Saihantala Depression, Erlian Basin. Master's Thesis, Northeast Petroleum University, Daqing, China, 2020.
57. Zhang, Y.M.; Liu, Z.; Fu, S.; Jiang, S.Q.; Yao, N.; Wang, X. New understandings of the basement characteristics and evolution process of Erlian Basin. *Oil Geophys. Prospect.* **2019**, *54*, 404–416.
58. Wu, P. The hydrocarbon accumulation mechanism of typical depression troughs in Erlian Basin. Ph.D. Thesis, China University of Geosciences, Beijing, China, 2020.
59. Zhao, X.Z.; Wang, Q.; Dan, W.N.; Wang, W.Y.; Qiao, X.X.; Ren, C.L. Exploration discovery and prospects of Cretaceous stratigraphic-lithologic reservoirs in Erlian Basin. *Lithol. Reserv.* **2017**, *29*, 1–9.
60. Li, J.H.; Hou, D.J.; Cao, L.Z.; Wu, P.; Zhao, Z.; Ma, X.X. Geochemical Characteristics and Source Correlation of Low-Mature Oil from the Tengge'er Formation (2^{nd} Member) in the Saihantala Sag, Erlian Basin. *Geoscience* **2021**, *35*, 315–325.
61. Cheng, S.Y.; Liu, S.F.; Su, S.; Ren, J.L. Structural characteristics analysis of Saihantala sag in Erlian Basin. *Oil Geophys. Prospect.* **2011**, *46*, 961–969.

62. Fu, S.; Liu, Z.; Ge, J.W.; Tian, N.; Wang, X.; Wang, H.L.; Liu, H.; Yin, K.W.; Han, Q. Tectono-stratigraphy characteristics of the Lower Cretaceous Saihantala Sag in the Erlian Basin, China: Normal faulting and controls on the depositional variability. *J. Pet. Sci. Eng.* **2020**, *195*, 107840. [CrossRef]
63. Qu, X.Y.; Yang, M.H.; Luo, X.H.; Ding, C.; Zhou, D.; Gong, T.; Yang, G. Extensional Tectonic Feature and Its Control on Hydrocarbon Accumulation of Saihantala Sag in Erlian Basin. *Geoscience* **2013**, *27*, 1023–1032.
64. Zou, C.N.; Zhao, Z.Z.; Yang, H.; Fu, J.H.; Zhu, R.K.; Yuan, X.J.; Wang, L. Genetic Mechanism and Distribution of Sandy Debris Flows in Terrestrial Lacustrine Basin. *Acta Sedimentol. Sin.* **2009**, *27*, 1065–1075.
65. Hart, B.S.; Plint, A.G. Gravelly Shoreface and Beachface Deposits. In *Sedimentary Facies Analysis*; Plint, A.G., Ed.; Wiley: Oxford, UK, 1995; Volume 22, pp. 75–99.
66. Massari, F.; Parea, G.C. Progradational gravel beach sequences in a moderate-to high-energy, microtidal marine environment. *Sedimentology* **1988**, *35*, 881–913. [CrossRef]
67. Miall, A.D. A review of the braided-river depositional environment. *Earth Sci. Rev.* **1977**, *13*, 1–62. [CrossRef]
68. Rust, B.R. Pebble Orientation In Fluvial Sediments. *J. Sediment. Petrol.* **1972**, *42*, 384–388.
69. Yang, K.; Zhu, X.M.; Liu, Y.; Liu, X.Z.; Guo, F. Key Signatures of Turbidite and Sandy Debris and Core Examples in Liaohe Basin. *J. Palaeogeogr. (Chin. Ed.)* **2020**, *22*, 483–492.
70. Covault, J.A.; Hubbard, S.M.; Graham, S.A.; Hinsch, R.; Linzer, H.-G. Turbidite-reservoir architecture in complex foredeep-margin and wedge-top depocenters, Tertiary Molasse foreland basin system, Austria. *Mar. Pet. Geol.* **2008**, *26*, 379–396. [CrossRef]
71. Orton, G.J.; Reading, H.G. Variability of Deltaic Processes in Terms of Sediment Supply, With Particular Emphasis on Grain Size. *Sedimentology* **1992**, *40*, 475–512. [CrossRef]
72. Blair, T.C.; McPherson, J.G. Grain-Size and Textural Classification of Coarse Sedimentary Particles. *J. Sediment. Res.* **1999**, *69*, 6–19. [CrossRef]
73. Li, H. Sedimentary Facies and Reservoir Characteristics of the Lower Cretaceous in Northern Area of Saihantala Sag. Master's Thesis, China University of Petroleum (East China), Qingdao, China, 2011.
74. Mc Pherson, J.G.; Shanmugam, G.; Moiola, R.J. Fan deltas and braid deltas: Varieties of coarse-grained deltas. *Geol. Soc. Am. Bull.* **1987**, *99*, 331–340. [CrossRef]
75. Hein, F.J.; Walker, R.G. Bar evolution and development of stratification in the gravelly, braided, Kicking Horse River, British Columbia. *Can. J. Earth Sci.* **1977**, *14*, 562–570. [CrossRef]
76. Miall, A.D. Lithofacies Types and Vertical Profile Models in Braided River Deposits: A Summary. In *Fluvial Sedimentology*; Miall, A.D., Ed.; Canadian Society of Petroleum Geologists: Calgary, AB, Canada, 1978; Volume 5, pp. 597–604.
77. Colella, A.; De Boer, P.L.; Nio, S.D. Sedimentology of A Marine Intermountain Pleistocene Gilbert-Type Fan-Delta Complex in The Crati Basin, Calabria, Southern Italy. *Sedimentology* **1987**, *34*, 721–736. [CrossRef]
78. Miall, A.D. Architectural-Element Analysis: A New Method of Facies Applied to Fluvial Deposits. *Earth Sci. Rev.* **1985**, *22*, 261–308. [CrossRef]
79. Yu, Z.; Chen, S.; Xie, W.; Zhao, S.e.; Ma, J.; Gong, T. Implication Linkage among Microfacies, Diagenesis, and Reservoir Properties of Sandstones: A Case Study of Dongying Formation, Nanpu Sag, Bohai Bay Basin. *Energies* **2022**, *15*, 7751. [CrossRef]
80. Schwartz, K.S. Bedform and Stratification Characteristic of Some Modern Small-Scale Washover Sand Bodies. *Sedimentology* **1982**, *29*, 835–849. [CrossRef]
81. Liu, E.; Deng, Y.; Lin, X.; Yan, D.; Chen, S.; Shi, X. Cenozoic Depositional Evolution and Stratal Patterns in the Western Pearl River Mouth Basin, South China Sea: Implications for Hydrocarbon Exploration. *Energies* **2022**, *15*, 8050. [CrossRef]
82. Ward, L.G.; Ashley, G.M. Introduction: Coastal lagoonal systems. *Mar. Geol.* **1989**, *88*, 181–185. [CrossRef]
83. Fawad, N.; Liu, T.; Fan, D.; Ahmad, Q.A. Sedimentary Facies Analysis of the Third Eocene Member of Shahejie Formation in the Bonan Sag of Bohai Bay Basin (China): Implications for Facies Heterogeneities in Sandstone Reservoirs. *Energies* **2022**, *15*, 6168. [CrossRef]
84. Zhao, Z.G.; Wang, F.Y.; Wang, H.B.; Wang, M.W.; Wang, H.; Lan, B.F. Source Kitchen and Organic Facies of Source Rocks in Saihantala Sag, Erlian Basin. *Lithol. Reserv.* **2017**, *29*, 28–35.
85. Maddy, D. An evaluation of climate, crustal movement and base level controls on the Middle-Late Pleistocene development of the River Severn, U.K. *Neth. J. Geosci.-Geol. Mijnb.* **2016**, *81*, 329–338. [CrossRef]
86. Yao, Z.Q.; Yu, X.H.; Shan, X.; Li, S.L.; Li, S.L.; Li, Y.L.; Tan, C.P.; Chen, H.L. Braided–meandering system evolution in the rock record: Implications for climate control on the Middle–Upper Jurassic in the southern Junggar Basin, north-west China. *Geol. J.* **2018**, *53*, 2710–2731. [CrossRef]
87. Ye, L.; Zhu, X.M.; Qin, Y.; Zhu, M. Depositional System of Shallow Water Delta in Rifted Lacustrine Basin. *J. Earth Sci. Environ.* **2018**, *40*, 186–202.
88. Jiang, Z.K.; Wang, Y.X.; Mao, Y.Q.; Zang, K.; Sun, W.; Liu, T.J. The relationship between paleoclimate change and paleosedimentary environment identification in coastal areas. *Arab. J. Geosci.* **2021**, *14*, 570. [CrossRef]
89. Fu, S.; Liu, Z.; Zhang, Y.M.; Wang, X.; Tian, N.; Yao, N.; Xiong, Y.; Chen, P.; Li, L.; Wang, H.L. Depositional systems and sequence stratigraphy of mesozoic lacustrine rift basins in NE China: A case study of the Wulan-Hua sag in the southern Erlian Basin. *J. Asian Earth Sci.* **2019**, *174*, 68–98. [CrossRef]
90. Mao, G.Z. Meso-Cenozoic Paleoclimate Evolution of Erlian Basin. *Energy Res. Manag.* **2015**, *4*, 92–96.

91. Tao, M.H.; Cui, Z.Q.; Chen, G.Q. Mesozoic Sporo-Pollen Assemblages and Climate Fluctuations in Northeast China. *Acta Micropalaeontol. Sin.* **2013**, *30*, 275–287.
92. Zhong, X.; Sun, X.C.; Gu, P.Y.; Li, X.Q.; Liu, S.; Liu, Y. Discovery and Paleoecological and Paleoenvironmental Environment of the Conchostracans from the Cretaceous Xiagou Formation in Zhangye National Geopark. *Acta Geosci. Sin.* **2020**, *41*, 543–553.
93. Meng, Q.R.; Hu, J.M.; Jin, J.Q.; Zhang, Y.; Xu, D.F. Tectonics of the late Mesozoic wide extensional basin system in the China–Mongolia border region. *Basin Res.* **2003**, *15*, 397–415. [CrossRef]
94. Wang, Y.Z. Coupling relationship of Mesozoic-Cenozoic Basin and Mountains in the Erlian Basin. *Spec. Oil Gas Reserv.* **2011**, *18*, 60–63, 138.
95. Xia, S.Q.; Lin, C.S.; Du, X.F.; Li, J.Q.; Li, H. Control of the Syndepositional Fault on Depositional Fillings of the Dongying Formation in Northern Liaodong Bay. *J. Southwest Pet. Univ. (Sci. Technol. Ed.)* **2020**, *42*, 19–32.